Supporting Information

Programming rigidity into size-defined wireframe DNA nanotubes

Daniel Saliba,[1,2] Xin Luo,[1,2] Felix J. Rizzuto,[1,3] and Hanadi F. Sleiman[1]*

[1] Department of Chemistry, McGill University, 801 Sherbrooke St. West, Montreal QC, H3A 0B8, Canada.

[2] These authors contributed equally.

[3] School of Chemistry, University of New South Wales, Sydney, 2052, Australia.

* E-mail: hanadi.sleiman@mcgill.ca

SI-1. Materials

Unless otherwise specified, all commercial reagents and solvents were used without additional purification. The following Sigma Aldrich products were used: magnesium chloride hexahydrate, sodium chloride, sodium citrate, and sodium hydroxide. Bioautomation supplied 1 μmol Universal 1000 Å LCAACPG supports and standard reagents for automated DNA synthesis. Fisher supplied the glacial acetic acid and boric acid. Biotium Inc. provided the GelRed™ nucleic acid dye. Bioshop Canada Inc. provided acrylamide/bis-acrylamide (40% 19:1 solution), ammonium persulfate, and tetramethylenediamine. New England Biolabs supplied T4 Polynucleotide Kinase (T4 PNK) and Quick T4 DNA ligase kits. FroggaBio provided MyTaq HS Red mix (Bioline). Qiagen's QIAquick gel extraction, QIAquick PCR purification, and QIAquick nucleotide purification kits were used to extract or clean PCR and temporal growth products.

1xTAMg buffer contains 45 mM Tris and 12.5 mM $MgCl_2.6H_2O$ with a pH of 8.0 adjusted with glacial acetic acid. 1xTBE buffer is composed of 90 mM Tris, 90 mM boric acid, and 2 mM

EDTA at a pH of 8.0. 1xSSC buffer is composed of 150 mM sodium chloride and 15 mM EDTA with a few drops of 1 M HCl to adjust the pH to 7.0. 1xTAE buffer contains 40 mM Tris, and EDTA at a pH of around 8.6. 1xALK buffer contains 30 mM sodium hydroxide and 2 mM EDTA at a pH of approximately 8.6.

SI-2. Instrumentation

Standard automated oligonucleotide solid-phase synthesis was performed on a Mermade MM6 Synthesizer from Bioautomation. PAGE was used to purify crude products with a length of less than 120 bases (20 x 20 cm vertical Hoefer 600 electrophoresis unit), whereas AGE was used to purify products with a length greater than 120 bases on an Owl Mini gel electrophoresis unit. UV absorbance measurements of DNA were acquired using a Thermo Scientific Nanodrop Lite spectrophotometer. Native PAGE experiments were performed employing a Bio-Rad Mini-PROTEAN Tetra Vertical Electrophoresis Cell. Gel images were taken using a Bio-Rad ChemiDoc™ MP System. We used an Eppendorf Mastercycler® 96 well thermocycler to conduct thermal annealing of DNA nanostructures, enzymatic reactions, and PCR. For air AFM measurements, Bruker ScanAsyst air probes with a nominal tip radius of 2 nm were utilized. Images of AFM were collected using a MultiMode8™ SPM linked to a Veeco Nanoscope™ controller.

SI-3. Oligonucleotide strands: synthesis, purification, and sequences

DNA synthesis and purification:

a. Non-modified DNA sequences

All strands were produced on a 1 μmol scale using a Mermade MM6 DNA synthesizer. The effectiveness of coupling was determined by removing the 5' DMT groups. The strands were deprotected and cleaved off the solid support in a concentrated ammonium hydroxide solution, followed by purification using denaturing PAGE (8 - 20% polyacrylamide/8M urea). Following electrophoresis, the required band was excised, crushed, and incubated overnight at 65 ^{o}C in 10 mL of autoclaved water. Concentrated to 1 mL, the material was then desalted using size exclusion chromatography (Sephadex desalting columns) and quantified using Nanodrop.

b. 5' phosphorylation of DNA sequences

Sequences used in the temporal growth process were phosphorylated using T4 Polynucleotide Kinase (T4 PNK). Each of the sequences involved was phosphorylated in 50 μL at a 500 pmol scale with 4 units of T4 PNK enzyme (incubation for 30 minutes at 37 ^{o}C and deactivation for 10 minutes at 65 ^{o}C).

SI-4. DNA sequences

a. Sequences for temporal growth backbones

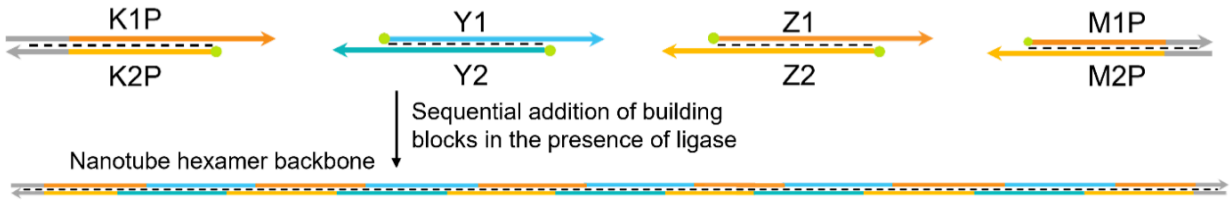

Figure S1. Nomenclature of DNA sequences used to form the temporal growth backbone for subsequent nanotube hexamer assembly. Phosphorylation of the K2P, Y1, Y2, Z1, Z2, and M1P sequences is shown by a green dot at the 5' end. The sequential addition of building blocks in the presence of quick ligase results in the generation of a backbone suitable for the assembly of a nanotube with six rung units.

Table S1. Temporal growth backbone oligonucleotide sequences used in the building of nanotubes with three and six rung units. All sequences are listed from 5' to 3' (5Phos = enzymatic phosphorylation).

Name	Sequence (5' → 3')
K1P	CTGGAGTCAACGCATCGAGATAGGTTAGTGGCGATACTAGGA
K2P	/5Phos/CAGCCAGATTTCCTAGTATCGCCACTAACCTATCTCGATG CGTTGACTCCAG
P1NT (forward)	CTGGAGTCAACGCATCG
P2NT (reverse)	/5Phos/TTGCAGGTGAATTCGGAC
M1P	/5Phos/AATCTGGCTGATGCTTTAGGAGAATAGCACATCTAGACTG GTATAGTCCGAATTCACCTGCAA
M2P	TTGCAGGTGAATTCGGACTATACCAGTCTAGATGTGCTATTCTCC TAAAGCAT
Y1	/5Phos/AATCTGGCTGATGCTTTAGGAATCAAACCAAAGTTCAGCA ACAGGCCGTTAAGGATCAGAAGAAATCTGGCTG
Y2	/5Phos/TCCTAAAGCATCAGCCAGATTTCTTCTGATCCTTAACGGC CTGTTGCTGAACTTTGGTTTGATTCCTAAAGCAT
Z1	/5Phos/ATGCTTTAGGAATCAAACCAAAGTTCAGCAACAGGCCGTT AAGGATCAGAAGA
Z2	/5Phos/CAGCCAGATTTCTTCTGATCCTTAACGGCCTGTTGCTGAA CTTTGGTTTGAT

b. Sequences for size defined DNA nanotubes

DNA sequences and general design of size-defined nanotubes assembled using type I rung units are presented in **Figure S2**. VXf, VXr, and Vm (orange strands) are the core strands forming the rung units onto which the other sequences hybridize to form a triangular rung. $R1_F$ and $R1_R$ hybridize to the 3' and 5' ends of the template, respectively, while $R1_M$ hybridizes to the middle part of the template. R1 and R2 are the rigidifiers that provide sticky ends for the rung unit from top and bottom. R1Xf, R2Xf, R1Xr, and R2Xr are rigidifiers used in the $R1_F$ and $R1_R$ assemblies that provide sticky ends for the rung unit from the top or bottom.

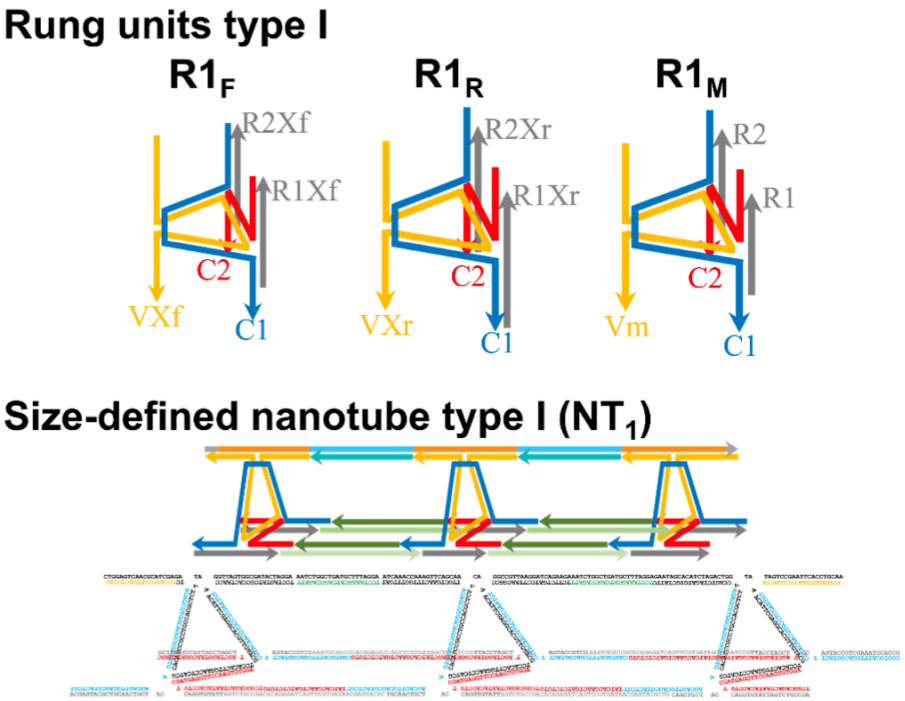

Figure S2. Sequence and general design of size-defined nanotubes type I (**NT$_1$**). DNA sequences forming several sorts of rungs units and the strands forming the entire nanotube are depicted schematically. Rungs R1$_F$ and R1$_R$ are the units that hybridize to the template's 3' and 5' ends, respectively, while R1$_M$ hybridizes to the middle part of the template.

Table S2. Oligonucleotide sequences used in the assembly of **NT$_1$**. All sequences are listed from 5' to 3'.

Name	Sequence (5' → 3')
V1-Vm	TCTTCTGATCCTTAACGGCCAACATTCGAGGCACGTTGTACGTC CACACTTGGAACCTCATCGCACATCCGCCTGCCACGCTCTTTTG CTGAACTTTGGTTTGAT
V1-VXr	TTGCAGGTGAATTCGGACTAAACATTCGAGGCACGTTGTACGTC CACACTTGGAACCTCATCGCACATCCGCCTGCCACGCTCTTCCA GTCTAGATGTGCTATTC
V1-VXf	TCCTAGTATCGCCACTAACCAACATTCGAGGCACGTTGTACGTC CACACTTGGAACCTCATCGCACATCCGCCTGCCACGCTCTTTCT CGATGCGTTGACTCCAG
V1-C1	CGGTGCATTTCGACGGTACTTCGTACAACGTGCCTCGAATGT AGAGCGTGGCAGGCGGATGTGAAGCAGTTGCAGCGTACTCGT
V1-C2	TCGGCAGACTAATACACCTGTCGATGAGGTTCCAAGTGTGGATA GCTAGGTAACGGATTGAGC
V1-R1	TGCAACTGCTACCAGGTGTATT
V1-R2	TTACCTAGCTCCAGTACCGTCG
V1-R1Xr	TGCAACTGCTACCAGGTGTATTAGTCTGCCGA
V1-R2Xr	TTACCTAGCTCCAGTACCGTCGAAATGCACCG

V1-R1Xf	ACGAGTACGCTGCAACTGCTACCAGGTGTATT
V1-R2Xf	GCTCAATCCGTTACCTAGCTCCAGTACCGTCG
V1-1a	TCCTAAAGCATCAGCCAGATT
V1-LS1	AGTCTGCCGACACAGAGATCAGTTCGTGATAACGAGTACGC
V1-LS2	AAATGCACCGCACAGAGATCAGTTCGTGATAGCTCAATCCG
V1-LS1/2*	TATCACGAACTGATCTCTGTG

The nomenclature of rung units in **NT_2** nanotubes is identical to **NT_1**. The rung units that comprise this nanotube are made up of a circular DNA template (**Figure S4**, black strand, T1) onto which the remaining sequences hybridize. Similar to $R1_F$ and $R1_R$, $R2_F$ and $R2_R$ hybridize to the template's 3' and 5' ends, respectively, while $R2_M$ hybridizes to the template's middle region.

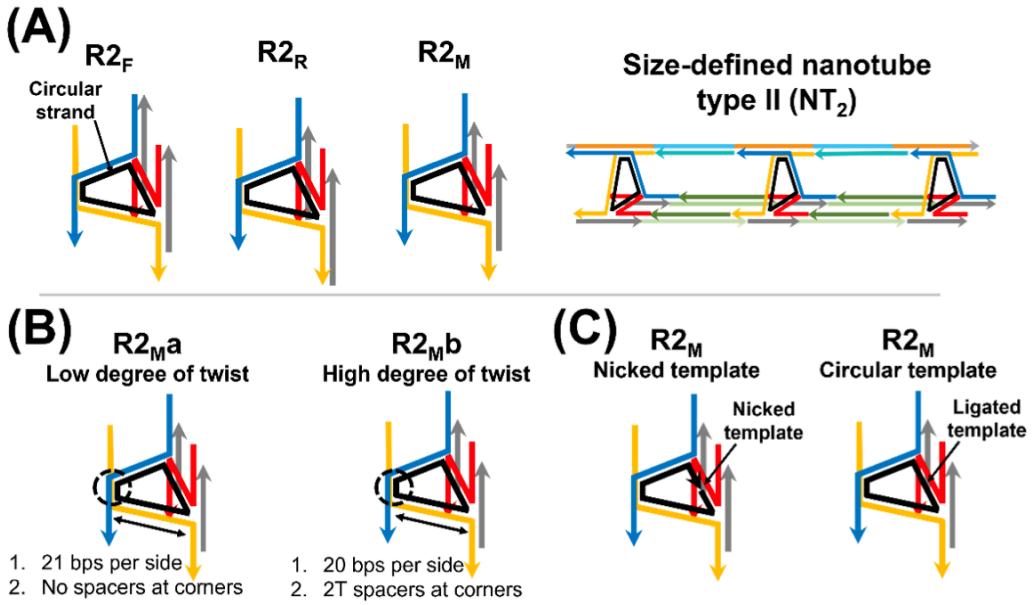

Figure S3. General design of size-defined nanotubes type II (**NT_2**). Rungs $R2_F$ and $R2_R$ are the units that hybridize to the 3' and 5' ends of the template, respectively, while $R2_M$ hybridizes to the middle part of the template (A). $R2_M$b with a low degree of twist consists of 21 bases per edge and no spacers at the corners of the circular template, whereas $R2_M$a with a high degree of twist consists of 20 bases per edge and 2 thymine at each corner of the circular template (B). $R2_M$ assembled with a nicked template and a circular template (black strands) (C).

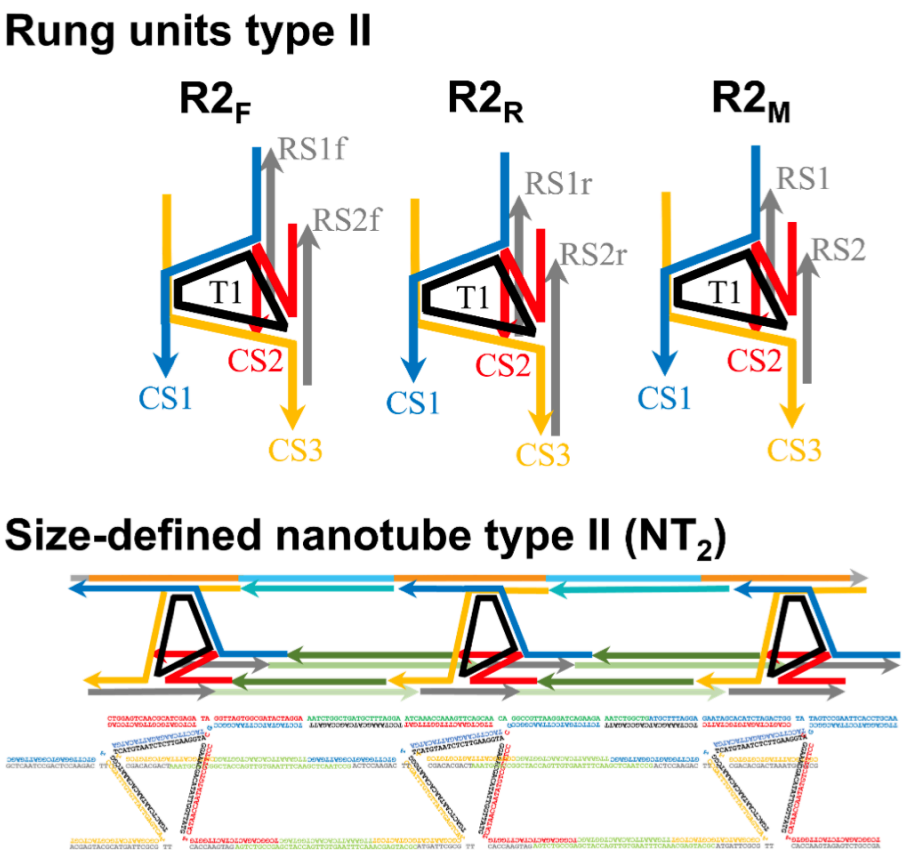

Figure S4. Sequence and general design of **NT₂**. DNA sequences forming several sorts of rungs units, in addition to the strands forming the entire nanotube, are depicted schematically. $R2_F$ and $R2_R$ are the units that hybridize to the 3' and 5' ends of the template, respectively, while $R2_M$ hybridizes to the middle part of the scaffold.

Table S3. Oligonucleotide sequences used in the assembly of **NT₂**. All sequences are listed from 5' to 3' (5Phos = enzymatic phosphorylation).

Name	Sequence (5' → 3')
V2-T1	/5Phos/TATTGGTTTGTGACCAATAACACAAATCGGTCAGTAATCT CTTGAAGGTAGGAAACGACA
V2-T1-2Tspacer	/5Phos/TATTGGTTTGTTTGACCAATAACACAAATCGGTTTCAGTAA TCTCTTGAAGGTATTGGAAACGACA
V2-CS1	TCTTCTGATCCTTAACGGCCTACCTTCAAGAGATTACTGAGTCTT GGAGTCGGATTGAGC
V2-CS2	TCGGCAGACTCTACTTGGTGCAAACCAATATGTCGTTTCCTTGCT GAACTTTGGTTTGAT
V2-RS1	ACTCCAAGACTTCGACACGACT
V2-RS1f	ACTCCAAGACTTGCTCAATCCGACTCCAAGAC
V2-RS1r	ACTCCAAGACTTCGACACGACTAAATGCACCG
V2-RS2	ATGATTCGCGTTCACCAAGTAG
V2-RS2f	ACGAGTACGCATGATTCGCG TT CACCAAGTAG

V2-RS2r	ATGATTCGCGTTCACCAAGTAGAGTCTGCCGA
V2-LS1	AGTCTGCCGAGCTACCAGTTGTGAATTTCAAACGAGTACGC
V2-LS2	AAATGCACCGGCTACCAGTTGTGAATTTCAAGCTCAATCCG
V2-LS1/2*	TTGAAATTCACAACTGGTAGC
V2-1a	TCCTAAAGCATCAGCCAGATT
V2-CS1 21bp 1un	TCTTCTGATCCTTAACGGCCGTACCTTCAAGAGATTACATGATGT CTTGGAGTCGGATTGAGC
V2-CS1-F 21bp 1un	TCCTAGTATCGCCACTAACCGTACCTTCAAGAGATTACATGATGT CTTGGAGTCGGATTGAGC
V2-CS1-R 21bp 1un	TTGCAGGTGAATTCGGACTAGTACCTTCAAGAGATTACATGATGT CTTGGAGTCGGATTGAGC
V2-CS2 21bp 1un	TCGGCAGACTCTACTTGGTGTCATAACCAATATGTCGTTTCCCTT GCTGAACTTTGGTTTGAT
V2-CS2-F 21bp 1un	TCGGCAGACTCTACTTGGTGTCATAACCAATATGTCGTTTCCCTC TCGATGCGTTGACTCCAG
V2-CS2-R 21bp 1un	TCGGCAGACTCTACTTGGTGTCATAACCAATATGTCGTTTCCCCC AGTCTAGATGTGCTATTC
V2-CS3	CGGTGCATTTAGTCGTGTCGCCGATTTGTGTTATTGGTCACGCG AATCATGCGTACTCGT
V2-CS3 21bp 1un	CGGTGCATTTAGTCGTGTCGTCCGATTTGTGTTATTGAGTCATCG CGAATCATGCGTACTCGT
V2-T1 21bp 1un	/5Phos/TATTGGTTTGTGACCAATAACACAAATCGGTCAGTAATCT CTTGAAGGTAGGAAACGACA
V2-splint T1 21un	TCACATAACCAATATGTCGTTTCCTAC
V2-T1 21bp 1un 2T spacer	/5Phos/TATTGGTTTGTTTGACCAATAACACAAATCGGTTTCAGTAA TCTCTTGAAGGTATTGGAAACGACA
V2-DX-1X-Z	GCGAAAGAGATTACGGCGACTCATCCGCGTAGCTCATTGGCT
V2-DX-1X-MZ1	GTGGAGCCAATGAGCTACTCTAGATGTGCTATTC
V2-DX-1X-MZ2	ACCAGGCGGATGAGTAACCT
V2-DX-1X-MZ3	TCTTCTGATCGCCACTCGCCGTAATCTCTT

The design and nomenclature of **NT_3** (**Figure S5**) are identical to those of **NT_2**, except that the backbone is composed of DX tiles rather than double-stranded DNA.

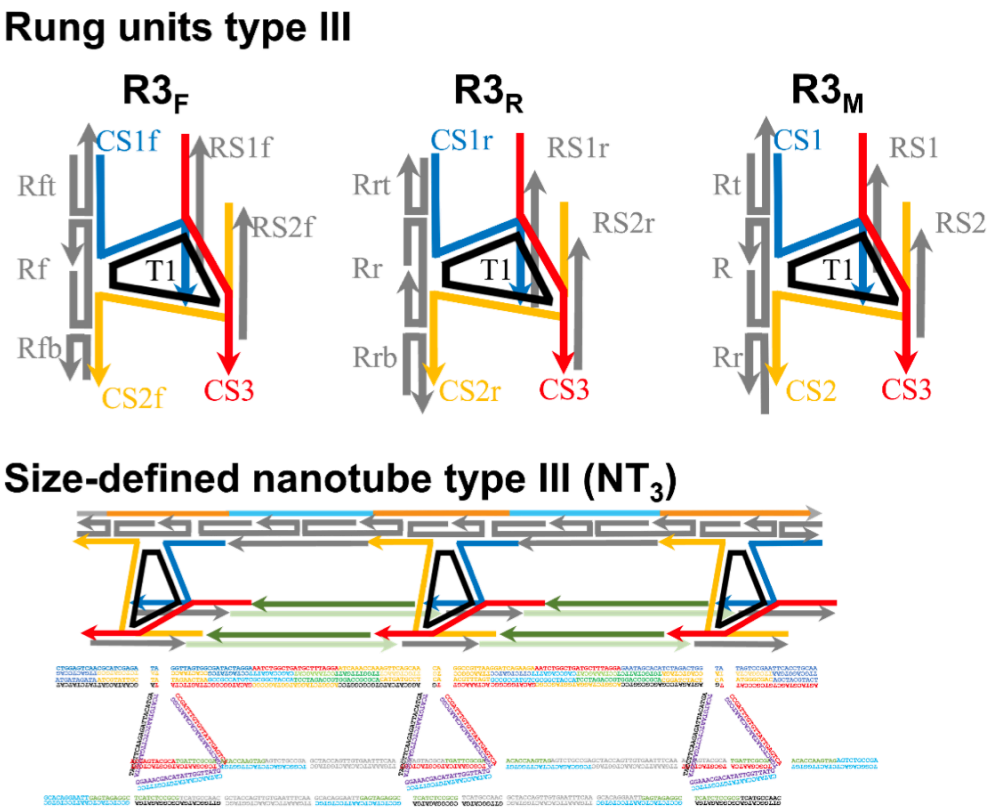

Figure S5. Sequence and general design of size-defined nanotubes type III (**NT$_3$**). DNA sequences forming several sorts of rungs units and the strands forming the entire nanotube are depicted schematically. R3$_F$ and R3$_R$ are the units that hybridize to the template's 3' and 5' ends, respectively, while R3$_M$ hybridizes to the middle part of the template.

Table S4. Oligonucleotide sequences used in the assembly of **NT$_3$**. All sequences are listed from 5' to 3' (5Phos = enzymatic phosphorylation).

Name	Sequence (5' → 3')
V3-DX-T1	/5Phos/TATTGGTTTGTGACCAATAACACAAATCGGTCAGTAATCT CTTGAAGGTAGGAAACGACA
V3-DX-CS1	GTTGGCATGACGCGGAGATGATACCTTCAAGAGATTACATGAGA GGCATCATGTGCGCGGTCC
V3-DX-CS1r	GTTGGCATGACGCGGAGATGATACCTTCAAGAGATTACATGAGA GTAGATCCGAGCGCGGTCC
V3-DX-CS1f	GTTGGCATGACGCGGAGATGATACCTTCAAGAGATTACATGAAG CAATACGATTATCTATCAT
V3-DX-CS2	GACATGGCGGCACTAAACGTTCCGATTTGTGTTATTGAGTCATC GCGAATCATGCGTACTCGT
V3-DX-CS2r	AGTACGTAGCTGTCGCCCATTCCGATTTGTGTTATTGAGTCATCG CGAATCATGCGTACTCGT
V3-DX-CS2f	GACATGGCGGCTTAGTTCTATCCGATTTGTGTTATTGAGTCATCG CGAATCATGCGTACTCGT

V3-DX-CS3	TCGGCAGACTCTACTTGGTGTCATAACCAATATGTCGTTTCCGCC TCTACTCAATTCCTGTGC
V3-DX-LS1	AGTCTGCCGAGCTACCAGTTGTGAATTTCAAACGAGTACGCA
V3-DX-LS2	TCATGCCAACGCTACCAGTTGTGAATTTCAAGCACAGGAATT
V3-DX-LS1/2*	TTGAAATTCACAACTGGTAGC
V3-DX-Rrt	TTGCAGGTGAAAGCTACGTACT
V3-DX-Rr	ACCAGTCTAGACGGATCTACTCAATGGGCGACTTCGGACTAT
V3-DX-Rrb	CCTAAAGCATTCCTAGACCGTGGACCGCGCTTGTGCTATTCT
V3-DX-Rft	CCTAGTATCGGCCGCCATGTCGCGGCTACCACAGCCAGATTT
V3-DX-Rf	ATCTCGATGCGATCGTATTGCTATAGAACTAACCACTAACCT
V3-DX-Rfb	ATGATAGATATTGACTCCAG
V3-DX-Rt	CTTCTGATCCGCCGCCATGTCGCGGCTACCACAGCCAGATTT
V3-DX-R	GTTGCTGAACTCATGATGCCTCAACGTTTAGTTTAACGGCCT
V3-DX-Rb	CCTAAAGCATTCCTAGACCGTGGACCGCGCATTGGTTTGATT
V3-DX-core	ACGGTCTAGGATGGTAGCCGC
V3-DX-dsR1	GAGTAGAGGCTCATCTCCGCG
V3-DX-dsR2	TGATTCGCGAACACCAAGTAG

SI-5. Production of size-defined templating strands with repetitive domains

The temporal growth approach employs sticky-ended dsDNA building units that are successively inserted with in-situ ligation to generate a full-length extended duplex. In summary, all component sequences with internal 5' ends were phosphorylated enzymatically at a concentration of 10 μM using T4 polynucleotide kinase (T4 PNK) (final mixture content: 2.5 mM ATP, 10 μM DNA, 1xT4 PNK buffer, and 0.08 U.μL^{-1} of T4 PNK). Following that, equal volumes of each complementary strand were combined and incubated at room temperature for 10 min. After adding an equal volume of 2xQuick ligase buffer, temporal growth was achieved by sequentially mixing an equal amount of duplex stocks as follows:

NT-6R backbone: a) K1P-K2P + Y1-Y2 + Quick ligase + Z1-Z2, b) M1P-M2P + Z1-Z2 + Quick ligase + Y1-Y2

To allow for both hybridization and ligation of the sticky ends of two consecutive building blocks, the mixture was incubated for 5 min following each addition of a building block. After adding the second building block, Quick ligase was added at an initial concentration of 10 U.μL^{-1}, and the mixture was incubated for 5 min. Following that, portions "a" and "b" were combined, incubated at room temperature for 15 minutes and loaded on a 2% native AGE (**Figure S6 (A)**). The full-length product was imaged under SYBR Safe channel, excised, and purified using QIAquick gel extraction Kit.

PCR reactions were carried out in batches of 200 μL each using MyTaq^{TM} HS Red Mix PCR Kit ([forward primer]$_{final}$ = [reverse primer]$_{final}$ = 0.625 μM, and a final concentration of 1xMyTaq™ HS Red Mix). The mixtures were heated at 95 ºC for 1 min, followed by 30 cycles of a) 95 ºC for 15 seconds, b) 64 ºC (optimized temperature for primer annealing) for 15 sec, and 3) 72 ºC for 15 sec. Next, the samples were purified by 2% denaturing AGE (1xALK, 2 h, 55 V), which was imaged under SYBR Gold channel (staining protocol: 1 min in distilled water, 15 min in 2xSSC, 15 min in 1xSSC and 1xSYBR Gold, and 15 min in 1xTAE) (**Figure S6 (B)**). Full-length backbones were excised and purified by Freeze 'N Squeeze™ DNA Gel Extraction Spin Columns (manufacturer protocol was applied).

PCR enrichment was performed with 5′-phosphorylated primers for the unwanted strand (**Figure S6 (C)**), followed by purification using PCR Purification kits. For the isolation of single-stranded templating strands, lambda exonuclease digestion was employed. Around 5000 ng of the obtained double-stranded PCR product was added to around 10 U of lambda exonuclease in 50 µL. The reaction mixture was incubated at 37 ºC for 30 min in 1xlambda exonuclease reaction buffer. The enzyme was heat-inactivated at 65 ºC for 30 min, and the resulting mixture

was used as a stock solution of the single-stranded templating backbone after being purified using a nucleotide cleaning Kit. The resultant ssDNA templates were quantified and visualized on native PAGE as indicated in **Figure S6 (D)**.

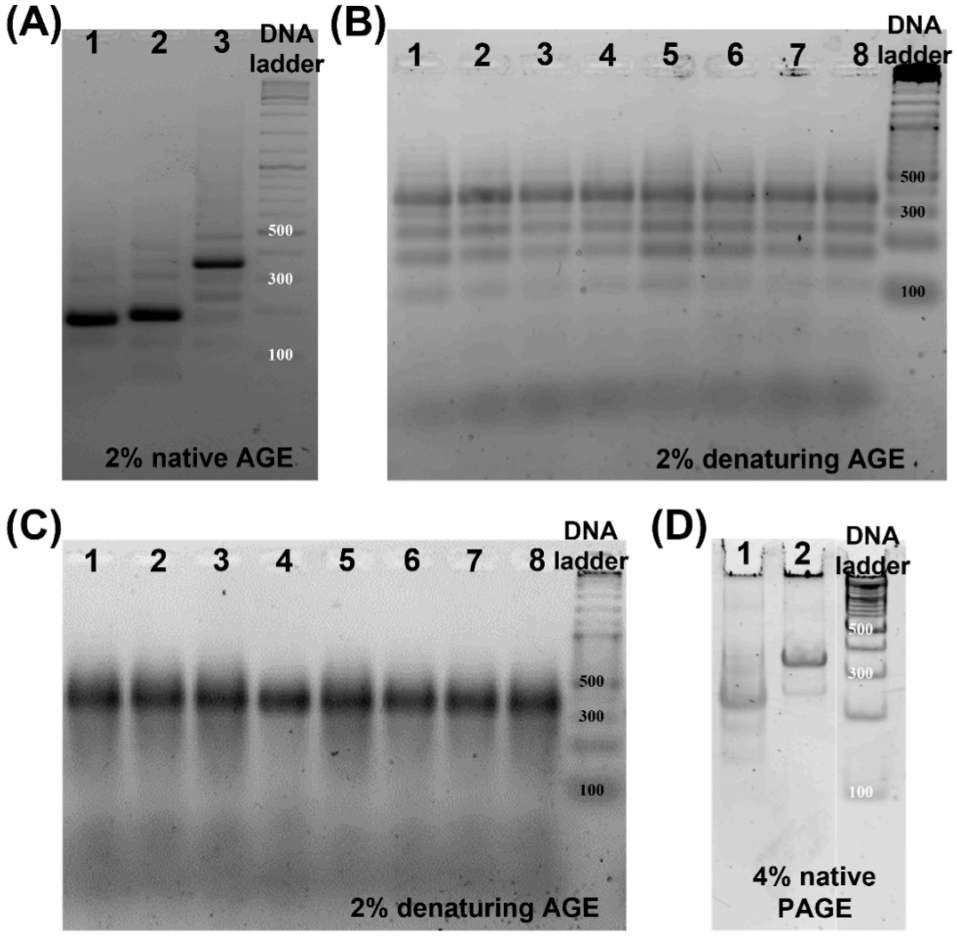

Figure S6. Temporal growth and optimization of the nanotube hexamer templating backbone through polymerase chain reaction. Temporal growth product of NT-6R is characterized by 2% native AGE. Lanes 1 and 2 represent fractions 1 and 2, respectively, whereas lane 3 represents the ligated combined product (lane 1 + lane 2) (NT-6R) (A). PCR optimization of the isolated NT-6R temporal growth strand. Lanes 1 to 4 contain a final template concentration of 0.15 ng.μL^{-1} and correspond to a primer annealing temperature of 63.5 ^{o}C, 64.8 ^{o}C, 65.1 ^{o}C and 66.5 ^{o}C, respectively. In lanes 5 to 8, similar primer annealing temperatures are employed, but the template concentration is 0.40 ng.μL^{-1} (B). PCR optimization of NT-6R following isolation and purification from the first round of PCR. Lanes 1 to 4 have a final template concentration of 0.05 ng.μL^{-1} and correspond to a primer annealing temperature of 64.9 ^{o}C,

65.5 °C, 65.9, and 66.4 °C, respectively. Similar primer annealing temperatures are used in lanes 5 to 8 but with a template concentration of 0.15 ng.μL^{-1} (C). Isolation of single-stranded NT-6R using lambda exonuclease. Lane 1 corresponds to the dsDNA treated with lambda exonuclease, and lane 2 to the dsNT-6R isolated from the second round of PCR. A band with an increased mobility shift is identified, indicating that the conversion to single-stranded NT-6R was effective (D).

SI-6. Assembly of size-defined DNA nanotubes

Each DNA triangular rung unit is formed by mixing all component strands in equimolar concentrations (check **Figure S2, Figure S4, and Figure S5** for nomenclature of sequences) to a final concentration of 0.5 μM in 1xTAMg. The mixture was annealed from 95 °C to 20 °C over 6 h resulting in a quantitative yield of the rung. The same procedure was used to generate double-stranded, partially double-stranded, and single-stranded linking strands, with a final concentration of 0.6 μM. Native PAGE (5%, 1xTAMg running buffer, stained with gel red) confirmed the clean formation of each product in quantitative yield, as it shown in **Figure S7, Figure S8,** and **Figure S9**. Note that the linking strands, backbone, and spacers used in assembling various types of nanotubes have the same sequence domains unless stated otherwise.

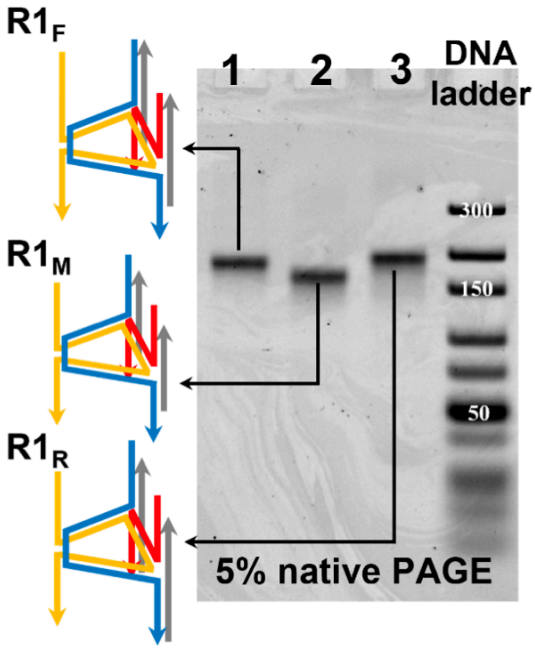

Figure S7. Assembly of type I rung units. Native PAGE analysis of $R1_F$, $R1_R$ and $R1_M$ rung units (lanes 1, 2, and 3, respectively). Rungs $R1_F$ and $R1_R$ are the units that hybridize to the 3' and 5' ends of the template, respectively, while $R1_M$ hybridizes to the middle part of the template. O'GeneRuler Ultra Low Range DNA ladder is used.

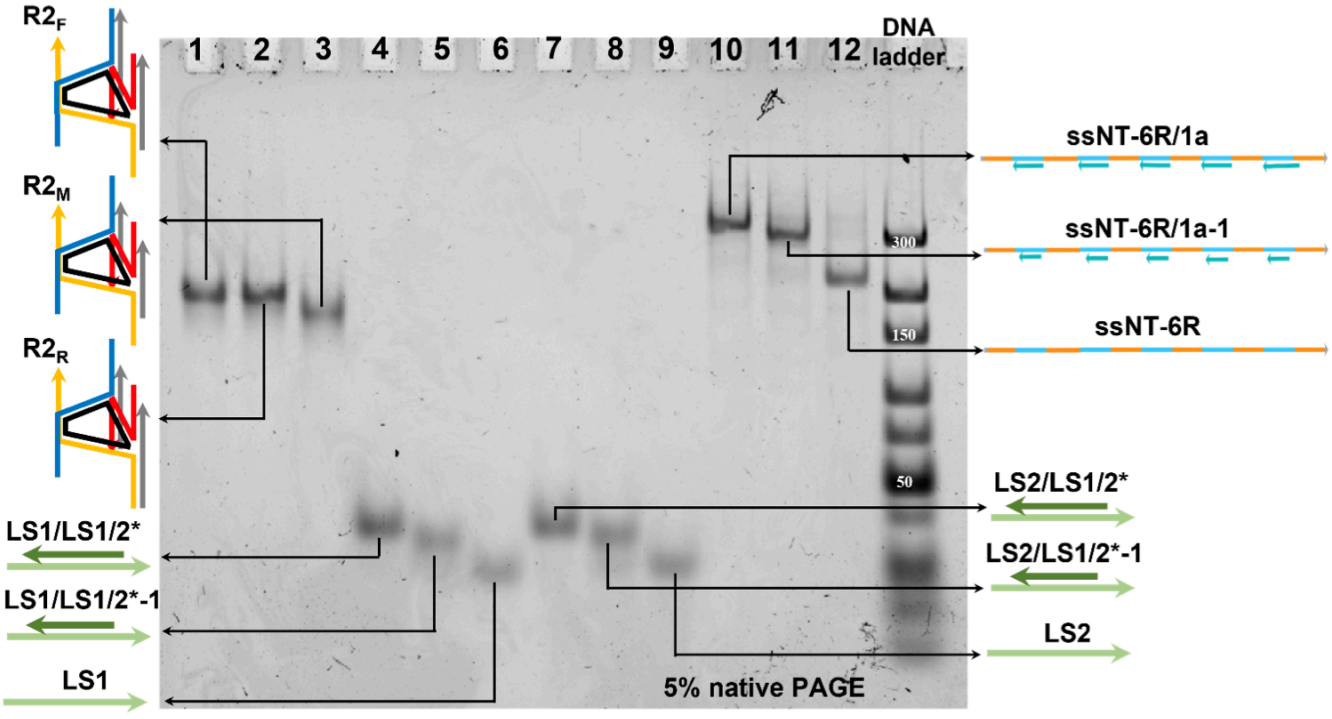

Figure S8. Characterization of circular templates and building blocks formation used in the assembly of **NT_2**. Native PAGE showing titration of linear template composed of 63 bases (21 bases per edge, 0 unhybridized bases at the corner) (lane 1) and linear template composed of

66 bases (20 bases per edge, 2 unhybridized bases at the corner) (lane 5) with the splint strand to give the circular product. Lanes 2 and 6 correspond to 0.5 eq of the splint, while lanes 3 and 7 correspond to 1 eq of splint, and lanes 4 and 8 correspond to 1.5 eq of splint. GeneRuler DNA ladder mix is used (A). Denaturing PAGE analysis of linear templates composed of 63 bases (21 bases per edge, 0 unhybridized bases at the corner) (lane 3) and linear templates composed of 66 bases (20 bases per edge, 2 unhybridized bases at the corner) (lane 4), each of which is incubated with 1 equivalent of splint strand, ligated using Quick ligase, and treated with exonuclease III and exonuclease I. Lanes 1 and 2 correspond to the 63 and 66 base circular products after exonuclease treatment, respectively (B). Native PAGE study of $R2_F$, $R2_R$ and $R2_M$ rung units built using a circular template (63 mer, 21 bases per edge, no corner spacers) (lanes 1, 2, and 3, respectively). Rungs $R2_F$ and $R2_R$ are the units that hybridize to the template's 3' and 5' ends, respectively, while $R2_M$ hybridizes to the template's middle section. Lanes 4 to 6 correspond to the first set of linking strands that produce a fully double-stranded, partially double-stranded, or single-stranded DNA nanotube; lanes 7 to 8 correspond to the second set of linking strands. Lanes 10 and 11 represent the annealing product of the template with a fully complement filler strand and one mismatch at each of its 5' and 3' ends. Lane 12 depicts the template in a single-stranded form. Same sets of linking strands and scaffolds were used in the assembly of **NT_2** and **NT_3**. O'GeneRuler Ultra Low Range DNA ladder is used (C).

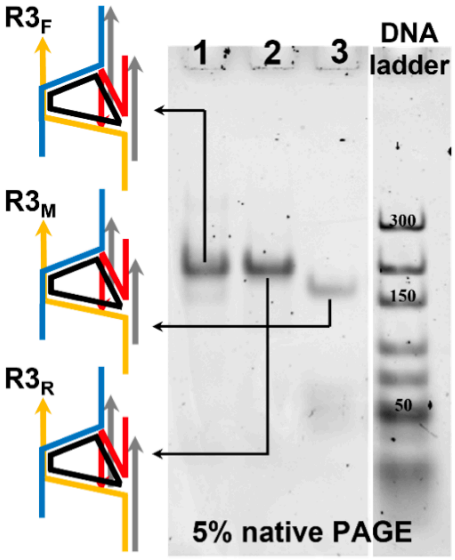

Figure S9. Assembly of type III rung units. Native PAGE analysis of $R3_F$, $R3_R$ and $R3_M$ rung units (lanes 1, 2, and 3, respectively). $R3_F$ and $R3_R$ are the units that hybridize to the 3' and 5' ends of the template, respectively, while $R3_M$ hybridizes to the middle part of the template. O'GeneRuler Ultra Low Range DNA ladder is used.

To form the size-defined nanotube hexamer, we combined the appropriate rung units (1 eq. of $R1_F$, 1 eq. of $R1_R$, and 4 eq. of $R1_M$) with the backbone and the spacer strand (5 eq. of 1a) to a final concentration of 50 nM in 1xTAMg. The mixture was annealed from 56 °C to 20 °C over 1 h to maximize efficient binding. The preorganized open assembly, constituted of a few rung units templated onto the backbone, was closed to the full nanotube after the addition of 5 equivalents of each of the two sets of linking strands (LS1 and LS2) and their complements (LS1/2*) while annealing the mixture from 44 to 20 °C over 4 h. Nanotube formation was characterized by a 1.5% AGE (1xTAMg running buffer, 55 V for 2 h) stained for 15 min in gel red. The assembly of fully double-stranded nanotubes employing type I rung units resulted in the production of a smeary band as detected by AGE (**Figure S10**, lane 1), but the assembly of partially double-stranded and single-stranded **NT_1**s resulted in the formation of a clean product band (**Figure S10**, lanes 2 and 3). AFM analysis revealed that fully double-stranded nanotubes form large aggregates (**Figure S11 (B)**), whereas partially double-stranded and single-stranded nanotubes produce collapsed structures (**Figure S13 (B)**).

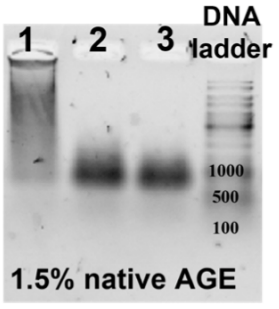

Figure S10. Assembly of single-stranded, fully double-stranded, and partially double-stranded nanotube hexamers (**NT_1**). Characterization of hexamer formation with native AGE (1xTAMg). Lanes 1, 2, and 3 correspond to DNA nanotube hexamers that are entirely double-stranded, partially double-stranded, or single-stranded, respectively. A fully dsDNA nanotube is formed by the addition of entirely complementary linking strands, whereas a partially double-stranded

DNA nanotube is formed by the addition of partially complementary linking strands. GeneRuler DNA ladder mix is used.

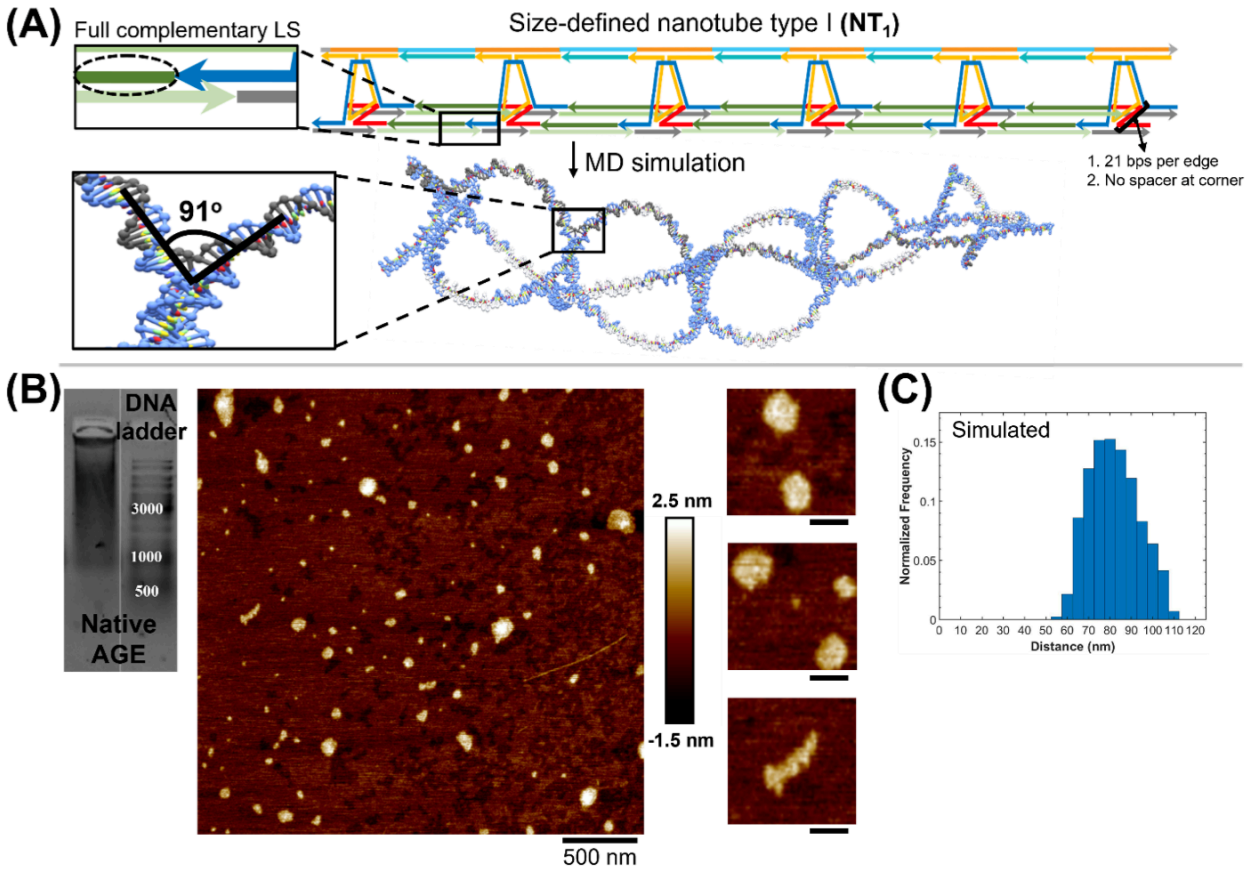

Figure S11. Schematic representation of fully double-stranded size-defined **NT$_1$** (**ds-NT$_1$**). Thermal annealing of five DNA strands yields the rung unit. The triangular units are then hybridized to the backbone, and the construction of the nanotube is completed by adding linking strands (A). Crosslinking is detected by AGE and AFM (B). MD simulations reveal a 91-degree twisting at the connection sites of the rungs to the backbone (A). Simulated (N = 2000, mean = 79 ± 12 nm) and experimental (aggregates were formed) maximum geometric distance of **ds-NT$_1$** (C). Scale bars are 500 nm and 90 nm.

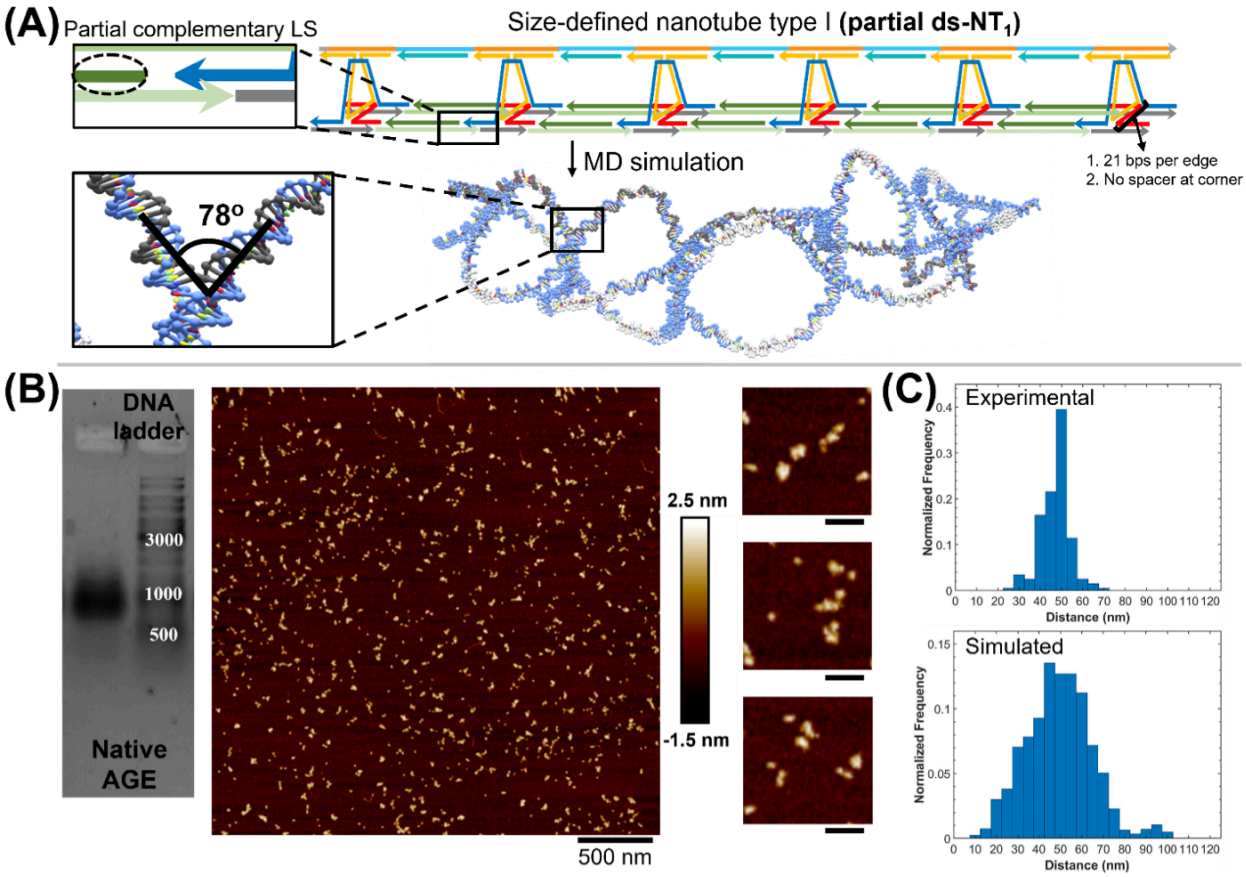

Figure S12. Schematic representation of a partially double-stranded size-defined DNA nanotube type I (**partial ds-NT$_1$**). The triangular units are hybridized onto the pillar and the construction of the nanotube is completed by adding partially complementary linking strands (A). MD simulations reveal a 78-degree angle between the rung overhangs below the triangular plane and those above the plane at the connection sites of the rungs to the pillar (A). AGE identifies a clean assembly, whereas collapsed structures are detected by AFM (B). Simulated (N = 2000, mean = 47 ± 16 nm) and experimental (N = 200, mean = 44 ± 7 nm) maximum geometric distance distributions of **partial ds-NT$_1$** are presented (C). Scale bars are 500 nm and 90 nm.

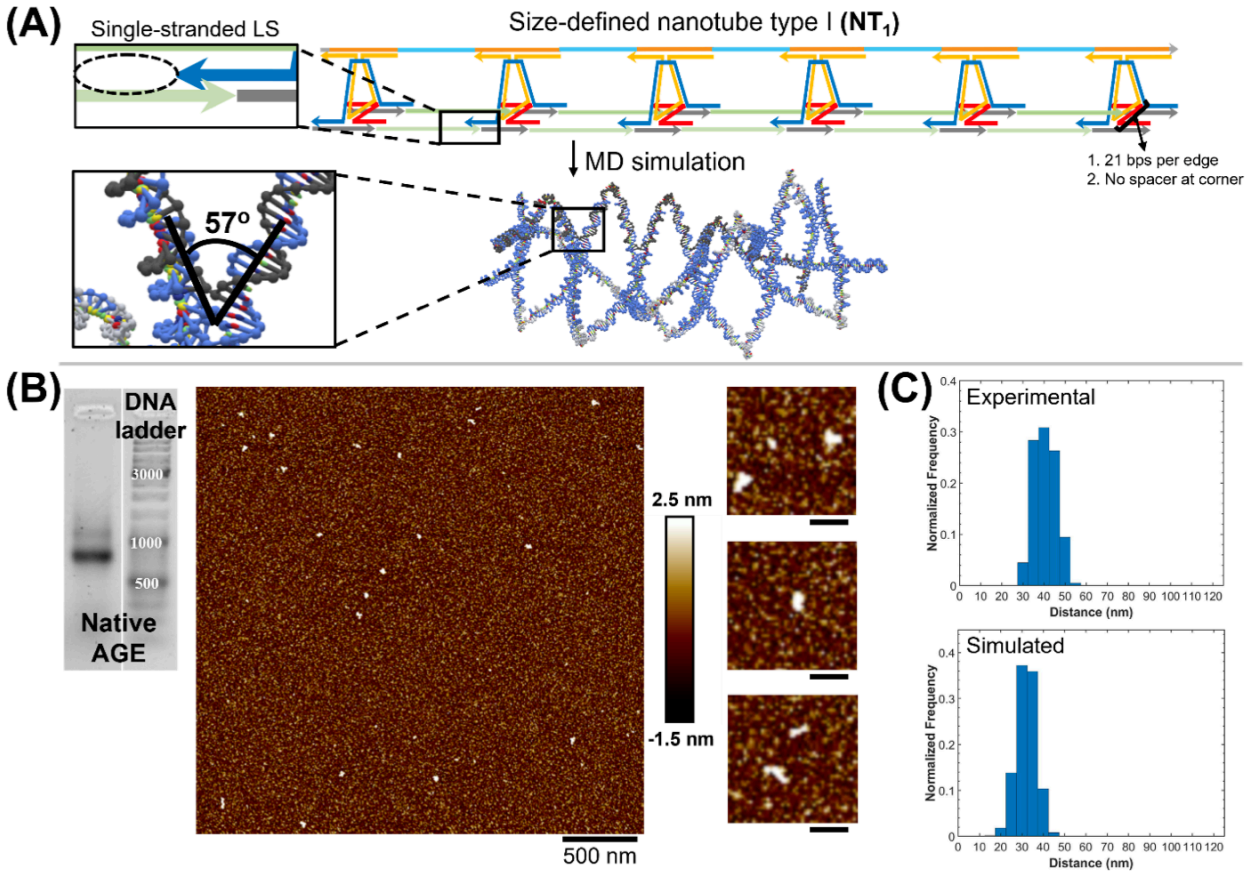

Figure S13. Schematic representation of single-stranded size-defined **NT₁** (**ss-NT₁**). The triangular units are hybridized into the backbone, and the construction of the nanotube is completed by adding single-stranded linking strands (A). MD simulations reveal a 57-degree angle between the rung overhangs below the triangular plane and those above the plane at the connection sites of the rungs to the backbone, in addition to a high degree of flexibility at the linking strand level (A). AGE identifies a clean assembly, whereas collapsed structures are detected by AFM (B). Simulated (N = 2000, mean = 30 ± 4 nm) and experimental (N = 200, mean = 37 ± 5 nm) maximum geometric distance of **ss-NT₁** (C). Scale bars are 500 nm and 90 nm.

Figure S14 illustrates a summary of the different strategies that were applied for the assembly of **NT₁**. Crosslinked products were formed when fully double-stranded linking strands are used, whereas distinct bands were formed when 1 or 2 bps were removed from each of the 5' and 3' ends of the complementary linking strands and spacer strands (dark green and dark blue strands). Nanotubes with DX tiles constructed at the backbone's spacer level and tubes with

varying spacing between two successive rung units showed similar effects. Finally, due to the tremendous degree of flexibility that single stranded DNA allows, using totally single-stranded connecting strands results in the production of monodispersed products that are completely collapsed.

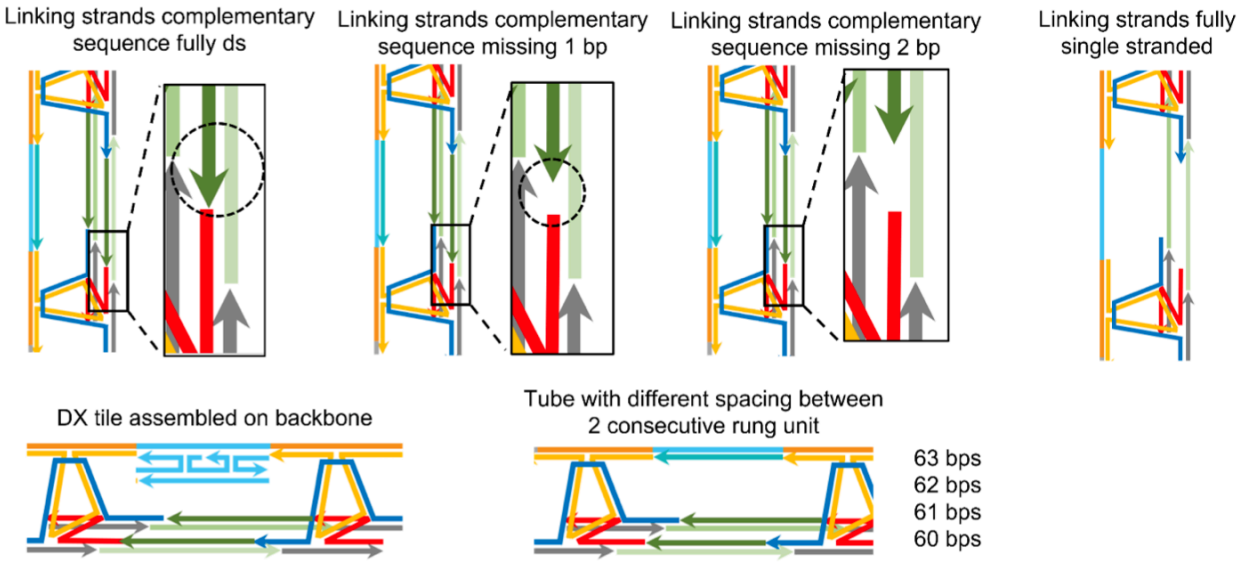

Figure S14. Different design strategies for the assembly of **NT_1**. **NT_1** assembled using fully double-stranded linking strands (A), partially double-stranded linking strands missing 1 base at each of the 5' and 3' ends of the complementary sequence (B), partially double-stranded linking strands missing 2 bases at each of the 5' and 3' ends of the complementary sequence (C), and single-stranded linking strands (D). **NT_1** assembled with DX tiles constructed at the backbone's spacer level (E), and DNA **NT_1** with varying spacing (63, 62, 61, and 60 bases) between two successive rung units (F).

The synthesis of nanotubes employing type II rung units followed the same technique as detailed previously, where an equimolar mixture of strands (CS1, CS2, CS3, RS1, RS2, and T, **Figure S4** and **Table S3**) was annealed in 1xTAMg. We were able to control the degree of twist of the rung units in this type of nanotube by varying two key parameters: i) the number of bases per rung edge (20 bps or 21 bps), and ii) the presence of a spacer on each of the

circular template's corners (2 thymine bases or no spacer) (**Figure S4**, black strand (T1)). Also, we examined the effect of using a circular template or relying on the circularization of the linear core strand during the annealing of the rung components. In the former case, the general approach applied in circularizing DNA strands consisted of using a splint-template strategy relying on the phosphorylation of the template, followed by splint addition, ligation, and enzymatic treatment with exonucleases. To do this, the 5' ends of the templates were phosphorylated enzymatically using T4 PNK at a concentration of 10 μM using T4 PNK (2.5 mM ATP, 10 μM DNA, 1xT4 PNK buffer, and 0.08 U.μL^{-1} of T4 PNK). Following that, one equivalent of splint strands was added, and the mixture was annealed in 1xTAMg for 1 h from 95 ^{o}C to 4 ^{o}C and characterized by native PAGE (**Figure S8 (A)**). The circular products were then ligated with Quick ligase at a concentration of 20 U/μL. The splint strand and linear templates were next digested with Exonuclease III and I, which selectively digest blunt or recessed 3′- termini. The cyclic product was subsequently isolated by denaturing PAGE (**Figure S8 (B)**), which had a higher mobility shift than cyclic products with more than one template strand domain (cyclic dimers and trimers). Native PAGE (5%, 1xTAMg running buffer, stained with gel red) confirmed the clean formation of rung units assembled with circular or non-circular templates (**Figure S15**).

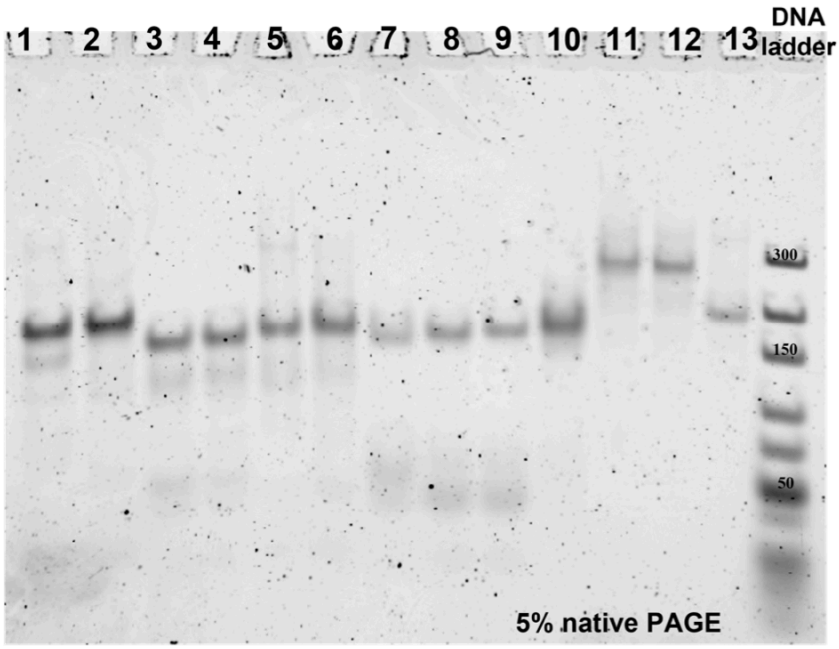

Figure S15. Building block assemblies used in the formation of size-defined **NT_2** (rungs with different circular and non-circular templates). Native PAGE study of $R2_F$ and $R2_R$ rung units constructed using a circular template (63 mer, 21 bases per edge, no corner spacers) (lanes 1 and 2, respectively). $R2_F$ and $R2_R$ are the units that hybridize to the 3' and 5' ends of the template, respectively. Lanes 3-6 correspond to the rung that hybridizes to the template's middle section ($R2_M$) when assembled with a non-circular template composed of 60 bases (20 bases per edge, 0 unhybridized bases at the corner), 66 bases (20 bases per edge, 2 unhybridized thymine bases at the corner), 63 bases (21 bases per edge, 0 unhybridized bases at the corner), and 69 bases (21 bases per edge, 2 unhybridized thymine bases at the corner), respectively. As with lanes 3-6, lanes 7–10 illustrate the same types of rung units built using a circular template. Lanes 12 and 13 show the annealing products of the scaffold with a fully complement spacer strand and another with a mismatch at each of its 5' and 3' ends. Lane 14 illustrates the scaffold in its single-stranded configuration. O'GeneRuler Ultra Low Range DNA ladder is used.

The length of the rung edge (20 bps or 21 bps) and the presence or absence of a corner spacer on the core strand (2 thymine bases or no spacer) had a negligible influence on the assembly (**Figure S15**). We employed type II rung units assembled using a circular template to form size-defined nanotube hexamers. We combined the appropriate number of rung equivalents (1 eq. of $R2_F$, 1 eq. of $R2_R$, and 4 eq. of $R2_M$) with the backbone and the spacer

strand (5 eq. of 1a) to a final concentration of 50 nM in 1xTAMg. The mixture was annealed from 56 °C to 20 °C over 1 h. The nanotube was fully assembled after the addition of 5 equivalents of each of the two sets of linking strands (LS1 and LS2) and their complements (LS1/2*) while annealing the mixture from 44 to 20 °C over 4 h. Nanotube formation was characterized by a 1.5% AGE (1xTAMg running buffer, 55 V for 2 h) stained for 15 min in gel red (**Figure S16**). The faint band that has a lower mobility shift than that of the major product may be a subproduct resulting from the misfolding of some rung units into higher-order structures (faint band with a lower mobility in Figure S15, lanes 1 and 5).

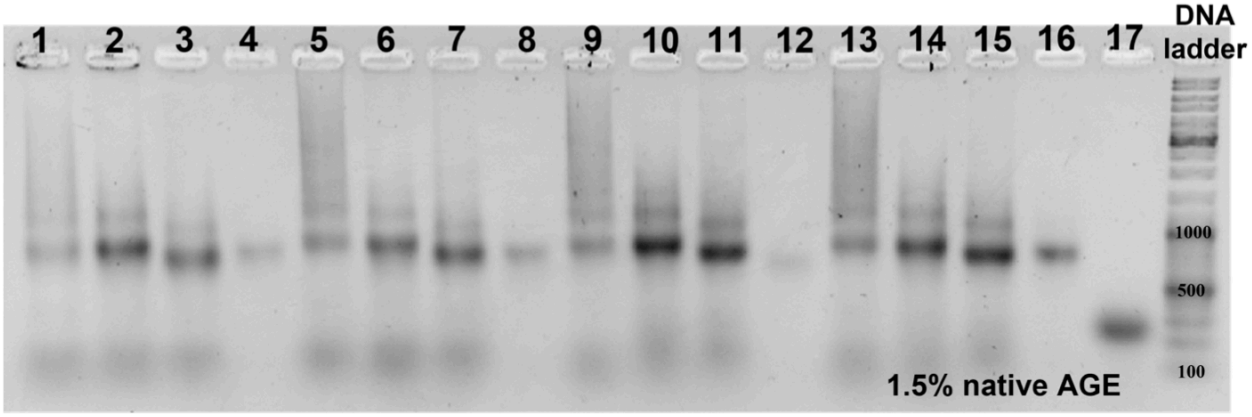

Figure S16. Assembly of **NT_2** using a circular template. Characterization of hexamer formation with native AGE (1xTAMg). Lanes 1-4 correspond to **NT_2** that are entirely double-stranded, partially double-stranded, single-stranded, or with no linking strands, respectively, assembled with rung units having 21 bases per edge and no spacers at the corners. Lanes 5-8 correspond to **NT_2** that are entirely double-stranded, partially double-stranded, single-stranded, or with no linking strands, respectively, assembled with rung units having 21 bases per edge and 2 thymine base spacers at the corners. Lanes 9-12 correspond to **NT_2** that are entirely double-stranded, partially double-stranded, single-stranded, or with no linking strands, respectively, assembled with rung units having 20 bases per edge and no spacers at the corners. Lanes 13-16 correspond to **NT_2** that are entirely double-stranded, partially double-stranded, single-stranded, or with no linking strands, respectively, assembled with rung units having 20 bases per edge and 2 thymine base spacers at the corners. Lane 17 represents the rung unit that hybridizes into the middle part of the backbone ($R2_M$). A fully dsDNA nanotube is

formed by adding entirely complementary linking strands, whereas a partially double-stranded DNA nanotube is formed by the addition of partially complementary linking strands. The mobility shift of nanotube hexamers with no linking strands is like that of nanotube hexamers with single-stranded linking strands, which could be due to a variation in shape that affects the structures' movement on AGE. GeneRuler DNA ladder mix is used.

With rung units containing 20 bases per edge and 2 thymine base spacers at the corner of the core template, fully double-stranded nanotubes form aggregates with some extended and collapsed nanotubes (**Figure S17**). When partially double- and single-stranded nanotubes are constructed using the same rung units, collapsed structures emerge (**Figure S18** and **Figure S19**). AFM analysis revealed that fully double-stranded nanotubes assembled using rung units having 21 bases per edge and no spacer at the corner of the core template form extended nanotubes with a certain degree of flexibility. Partially double-stranded and single-stranded nanotubes, assembled with the same rung units, produce structures with higher flexibility and collapsed structures, respectively (**Figure S21** and **Figure S22**). Since the nanotubes described in this manuscript are comprised of rung units with 21 bases per edge, the calculated diameter of the nanotube will equal the sum of the lengths of one edge and one double-stranded DNA helix that constitutes the nanotube main axis. This yields a total edge length of 8.8 nm.

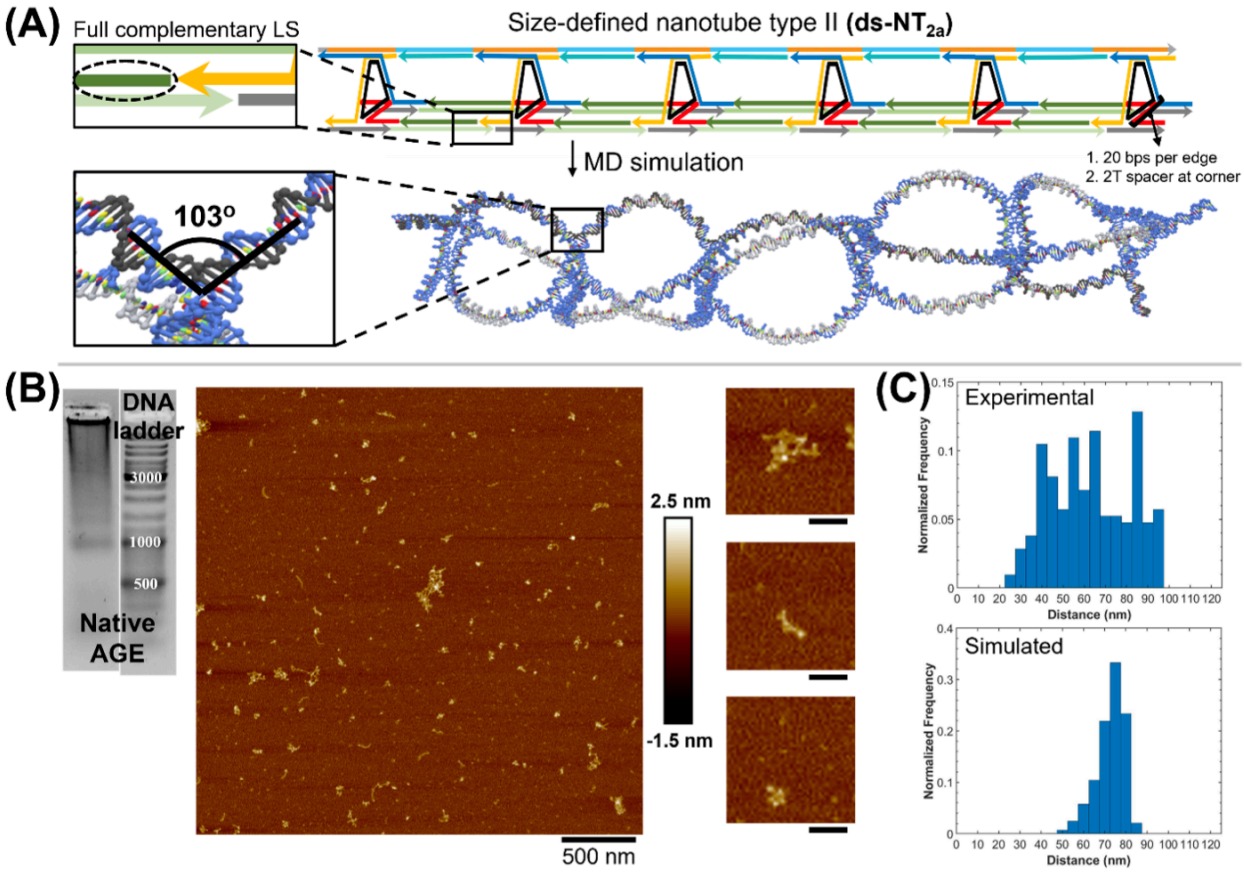

Figure S17. Schematic representation of a fully double-stranded size-defined **NT$_2$** (**ds-NT$_{2a}$**) (high twist rung). The rung unit is built by thermally annealing six DNA strands using a circular template (rung having 20 bps per edge and the circular template possessing 2 thymine bases as spacers at each corner). The triangular units are then hybridized into the backbone, and the nanotube is formed by adding linking strands that are fully double-stranded (A). MD simulations reveal a 103-degree angle between the rung overhangs below the triangular plane and those above the plane at the connection sites of the rungs to the backbone (A). Crosslinking is detected by AGE along with a faint band that corresponds to extended and collapsed size-defined nanotubes shown by AFM (B). Simulated (N = 2000, mean = 70 ± 7 nm) and experimental (N = 200, mean = 70 ± 21 nm) (along with the formation of some aggregates) maximum geometric distance distributions of **ds-NT$_{2a}$** assembled with a rung having a high degree of twist are presented (C). Scale bars are 500 nm and 90 nm.

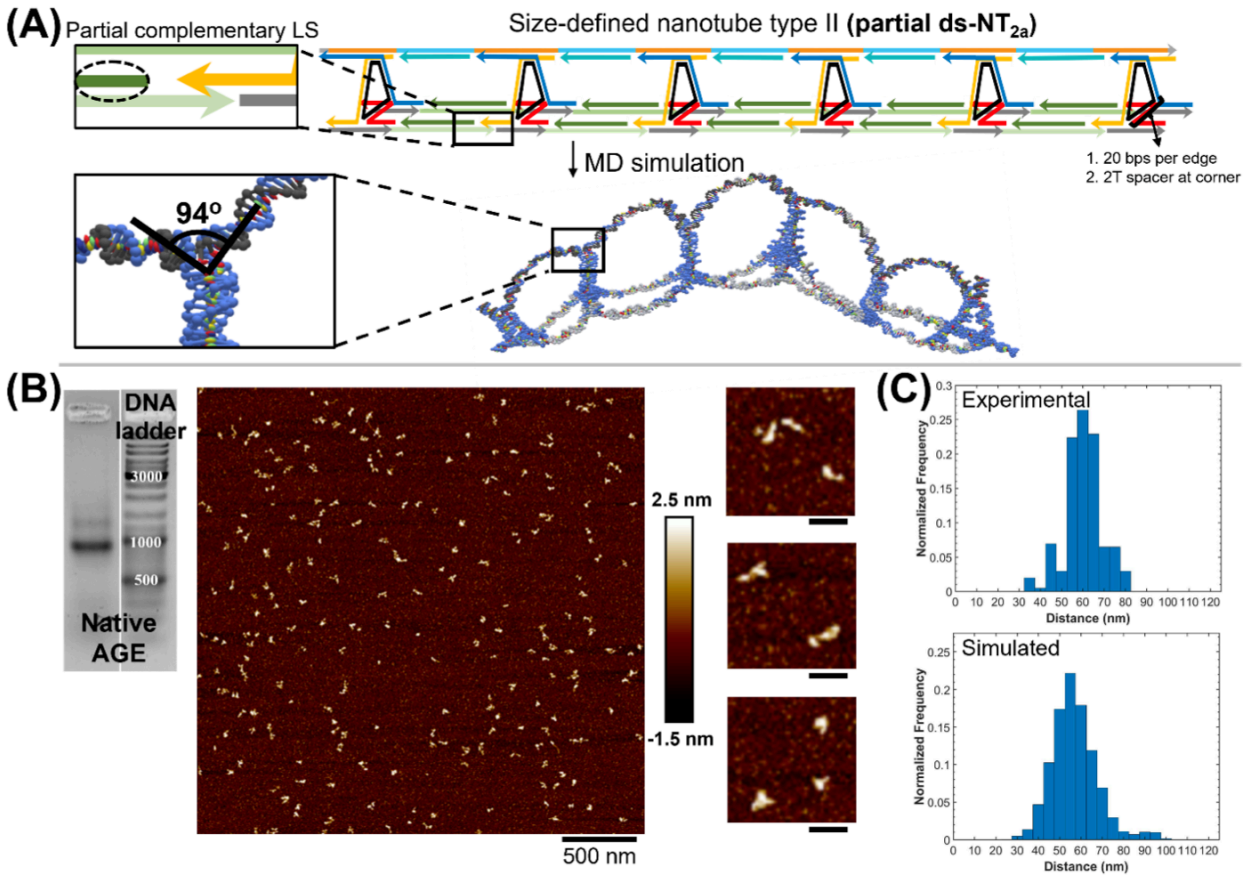

Figure S18. Schematic representation of a partially double-stranded size-defined **NT_2** (**partial ds-NT_{2a}**) (rung with a high degree of twist). The rung unit is built by thermally annealing six DNA strands using a circular template (rung having 20 bps per edge and the circular template possessing 2 thymine bases as spacers at each corner). After hybridizing the triangle units to the backbone, the nanotube is created by adding linking strands missing one base from both the 5' and 3' ends (A). MD simulations reveal a 94-degree angle between the rung overhangs below the triangular plane and those above the plane at the connection sites of the rungs to the backbone (A), resulting in predominantly collapsed structures as identified by AFM (B). AGE identifies a clean assembly (B). This type of nanotube has a lower degree of collapse than type I. Simulated (N = 2000, mean = 55 ± 10 nm) and experimental (N = 200, mean = 58 ± 9 nm) maximum geometric distance distributions of **partial ds-NT_{2a}** assembled with a rung having a high degree of twist are presented (C). Scale bars are 500 nm and 90 nm.

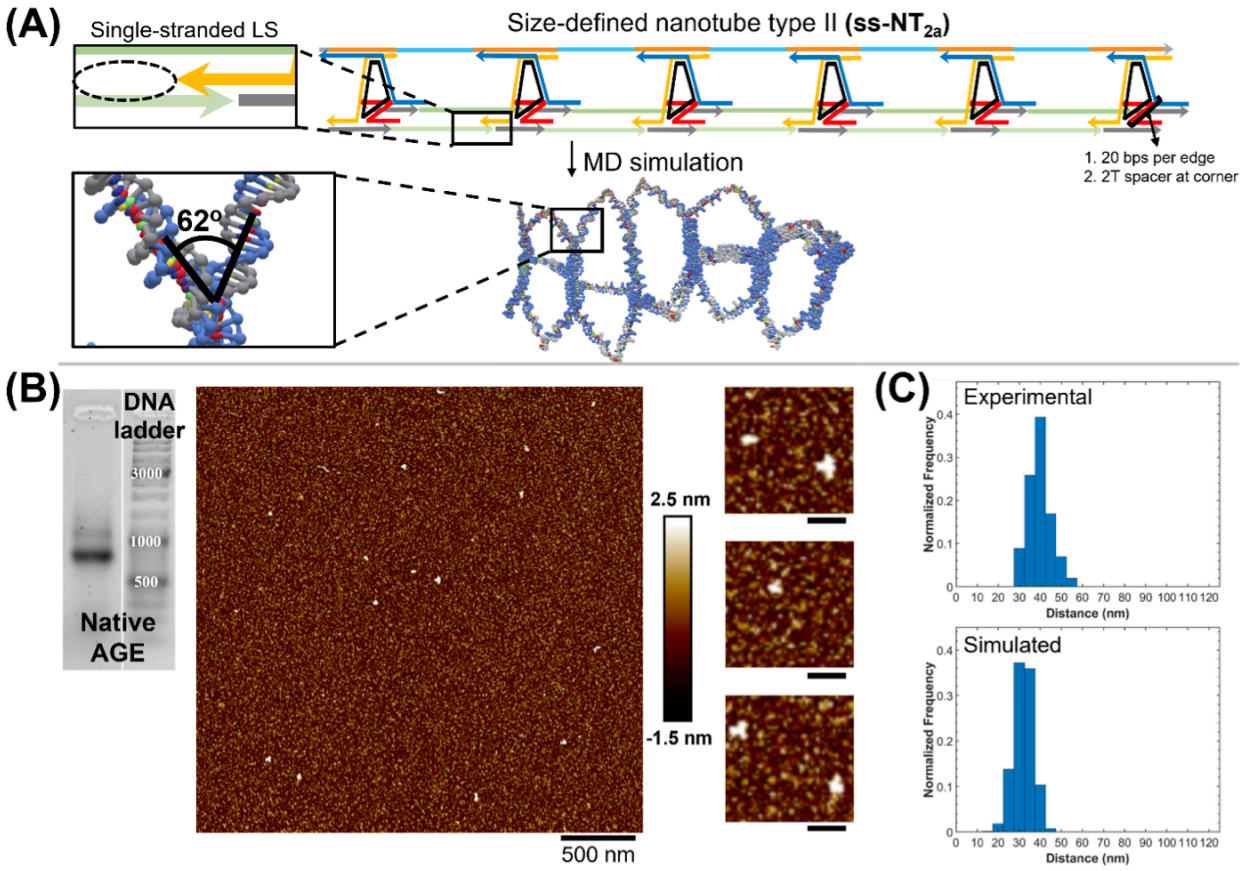

Figure S19. Schematic representation of a single-stranded size-defined **NT_2 ($ss\text{-}NT_{2a}$)** (rung with a high degree of twist). Six DNA strands are thermally annealed together to form the rung unit using a circular template (rung having 21 bps per edge and the circular template possessing no spacers at the corner). After hybridizing the triangle units to the backbone, the nanotube is formed by adding single-stranded linking strands (A). While AGE identifies a clean assembly (B), MD simulations reveal a 62-degree angle between the rung overhangs below the triangular plane and those above the plane at the connection sites of the rungs to the backbone, in addition to a high degree of flexibility at the linking strand level (A), resulting in collapsed structures that are easily identified by AFM (B). Simulated (N = 2000, mean = 30 ± 4 nm) and experimental (N = 200, mean = 37 ± 6 nm) maximum geometric distance distributions of **$ss\text{-}NT_{2a}$** assembled with a rung having a high degree of twist are presented (C). Scale bars are 500 nm and 90 nm.

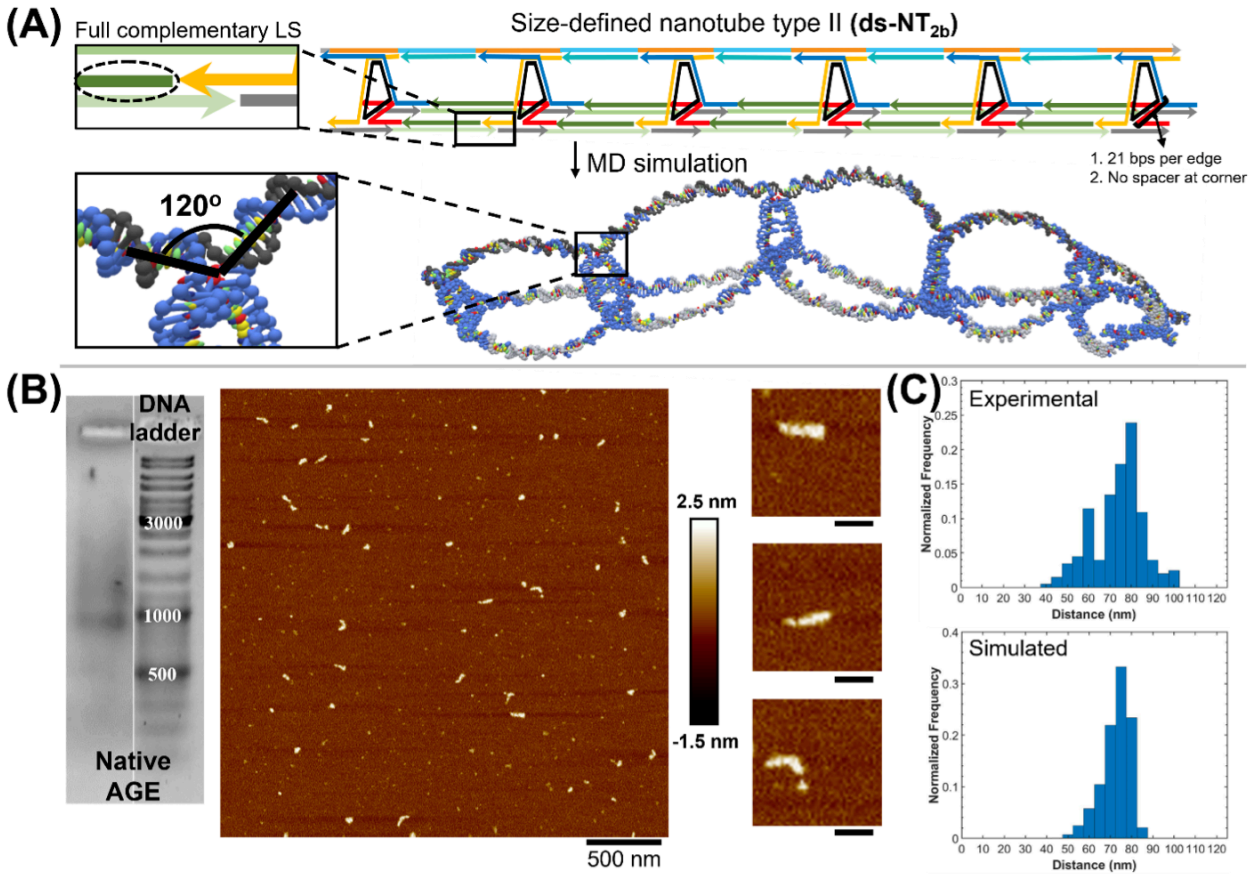

Figure S20. Schematic representation of a fully double-stranded size-defined DNA nanotube type II (rung with a low degree of twist) (**ds-NT$_{2b}$**). Using a circular template, six DNA strands are thermally annealed together to generate the rung unit (rung having 21 bps per edge and the circular template possessing no spacers at the corner). After hybridizing the triangle units to the pillar, the nanotube is constructed by adding fully complementary linking strands (A). MD simulations reveal a 120-degree angle between the rung overhangs below the triangular plane and those above the plane at the connection sites of the rungs to the pillar (A), leading to partially extended structures that are readily identifiable by AFM (B). AGE identifies a clean construction with a low degree of smearing (B). Simulated (N = 2000, mean length = 70 ± 7 nm) and experimental (N = 200, mean length = 70 ± 10 nm) maximum geometric distance distributions of **ds-NT$_{2b}$** assembled with a rung having a low degree of twist are presented (C). Scale bars are 500 nm for large AFM image and 90 nm for insets.

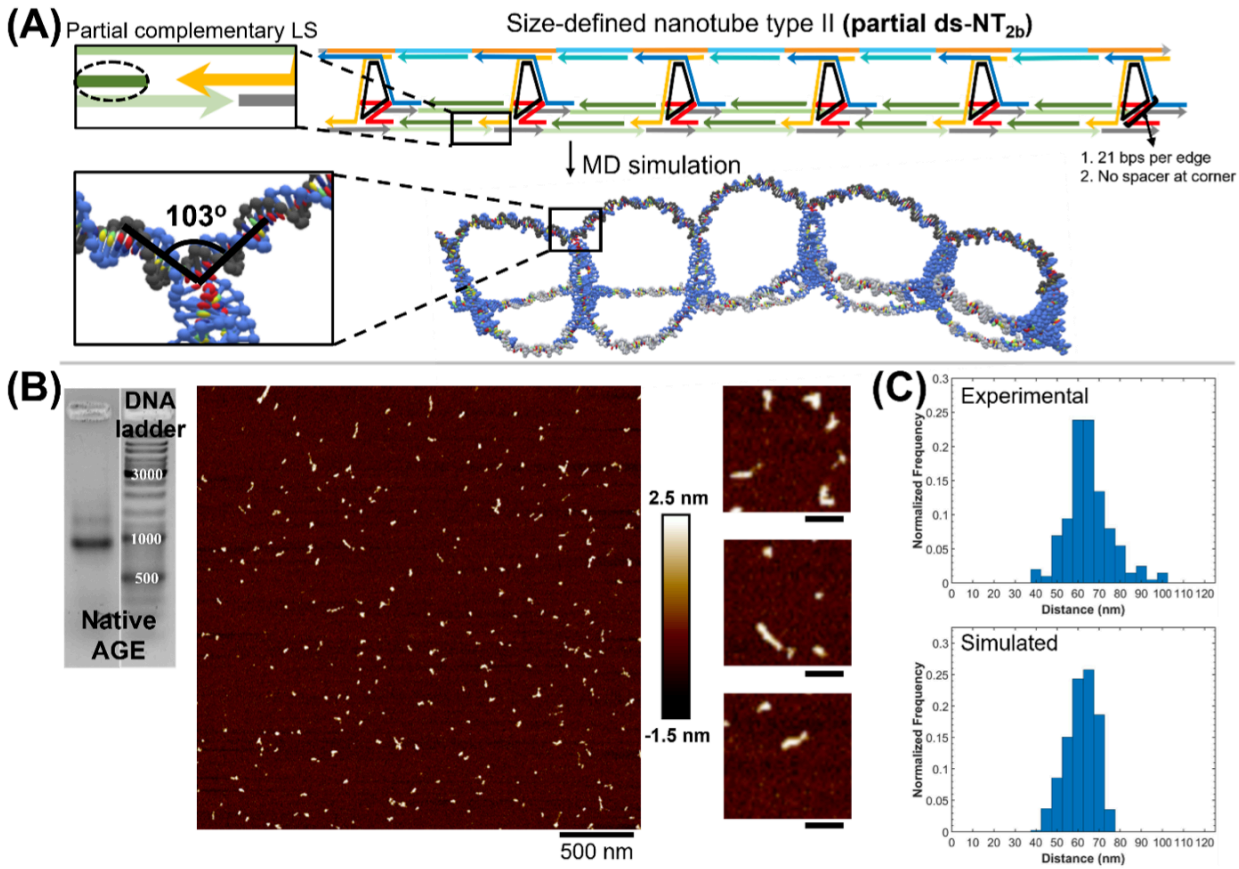

Figure S21. Schematic representation of a partially double-stranded size-defined **NT_2 (partial ds-NT_{2b})** (rung with a low degree of twist). Using a circular template, six DNA strands are thermally annealed together to generate the rung unit (rung having 21 bps per edge and the circular template possessing no spacers at the corner). After hybridizing the triangle units to the backbone, the nanotube is constructed by adding linking strands deficient in one base at both the 5' and 3' ends (A). While AGE identifies a clean construction (B), MD simulations reveal a 103-degree angle between the rung overhangs below the triangular plane and those above the plane at the connection sites of the rungs to the backbone, leading to collapsed and extended structures that are readily identifiable by AFM (B). Simulated (N = 2000, mean = 59 ± 7 nm) and experimental (N = 200, mean = 62 ± 11 nm) maximum geometric distance distributions of **partial ds-NT_{2b}** assembled with a rung having a low degree of twist are presented (C). Scale bars are 500 nm and 90 nm.

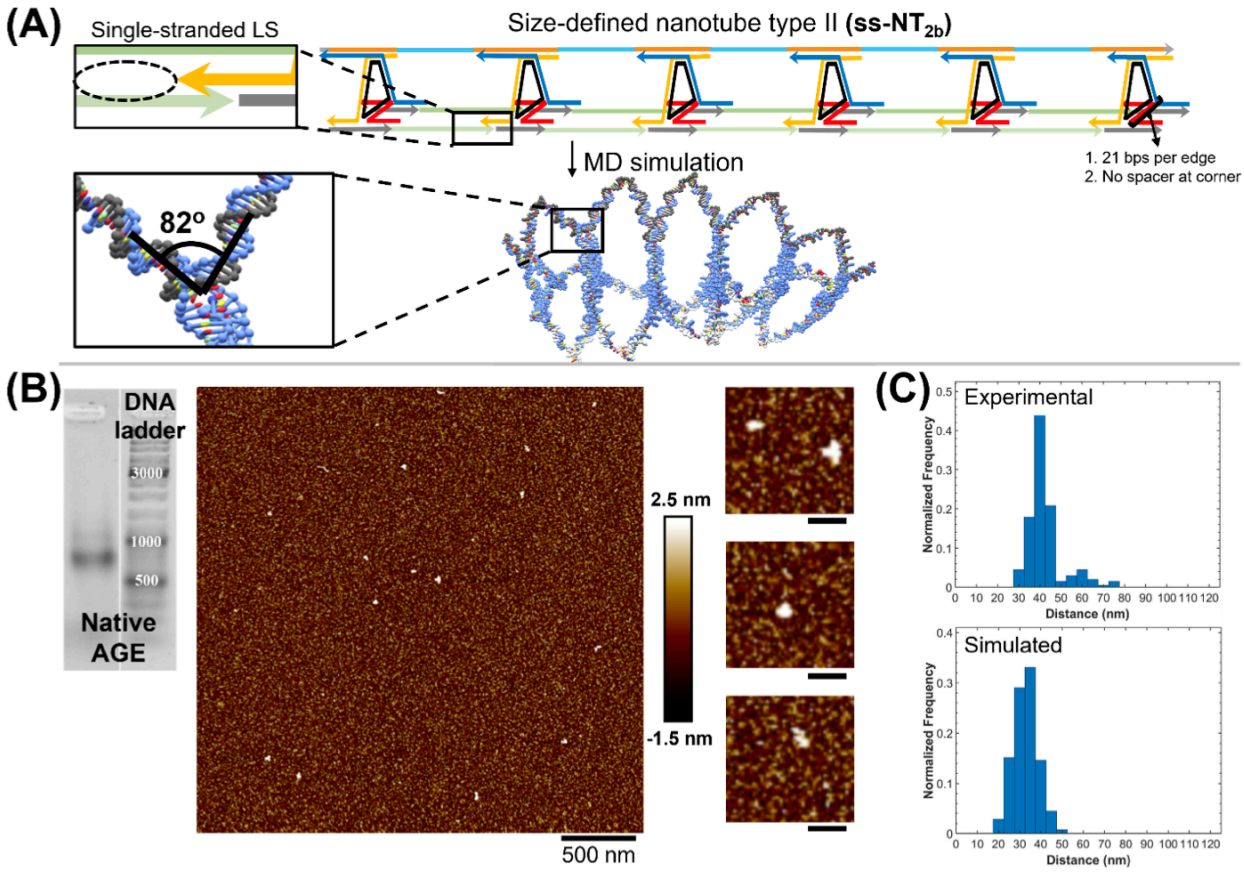

Figure S22. Schematic representation of a single-stranded size-defined **NT_2 (ss-NT_{2b})** (rung with a low degree of twist). The rung unit is built by thermally annealing six DNA strands using a circular template (rung having 21 bps per edge and the circular template possessing no spacers at the corner). The triangular units are then hybridized into the backbone, and the nanotube is formed by adding single-stranded linking strands (A). AGE detects a clean assembly (B), while MD simulations reveal an 82-degree angle between the rung overhangs below the triangular plane and those above the plane at the connection sites of the rungs to the backbone, as well as a high degree of flexibility at the linking strands level (A), resulting in collapsed structures as detected by AFM (B). Simulated (N = 2000, mean = 30 ± 6 nm) and experimental (N = 200, mean = 39 ± 8 nm) maximum geometric distance distributions of **ss-NT_{2b}** assembled with a rung having a low degree of twist are presented (C). Scale bars are 500 nm and 90 nm.

Rigid size-defined nanotube hexamers (**NT_3**) were assembled by annealing DX staple strands with the single-stranded scaffold. The proper number of equivalents of each staple was added in addition to the rung units' components (1 eq. of $R3_F$, 1 eq. of $R3_R$, and 4 eq. of $R3_M$), and the whole mixture was annealed from 95 °C to 4 °C for 4 hours in 1xTAMg. The nanotube's

closed-form was achieved after adding 5 equivalents of each of the two sets of linking strands (LS1 and LS2) and their complements (LS1/2*) while annealing the mixture from 44 to 20 ^{o}C over 4 h. Nanotube formation was characterized by a 1.5% AGE (**Figure S23**) (1xTAMg running buffer, 55 V for 2 h).

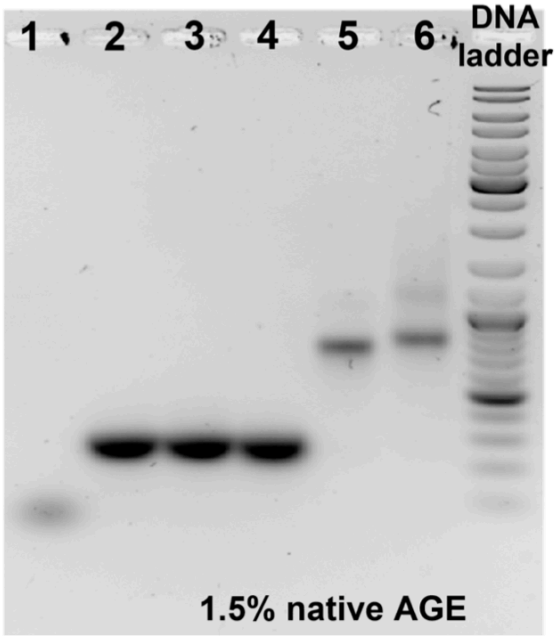

Figure S23. Nanotube hexamer assembly (type III). Hexamer formation characterization using native AGE (1xTAMg). Lane 1 represents the linking strands (LS1/LS1/2* and LS2/LS1/2*). Lanes 2, 3, and 4 correspond to rungs $R3_F$, $R3_R$, and $R3_M$, respectively. Lanes 5 and 6 represent the nanotube hexamer, with a DX backbone, formed by adding single-stranded linking strands and the nanotube hexamer formed by adding double-stranded linking strands, respectively. Rung units are assembled using a non-circular template. GeneRuler DNA ladder mix is used.

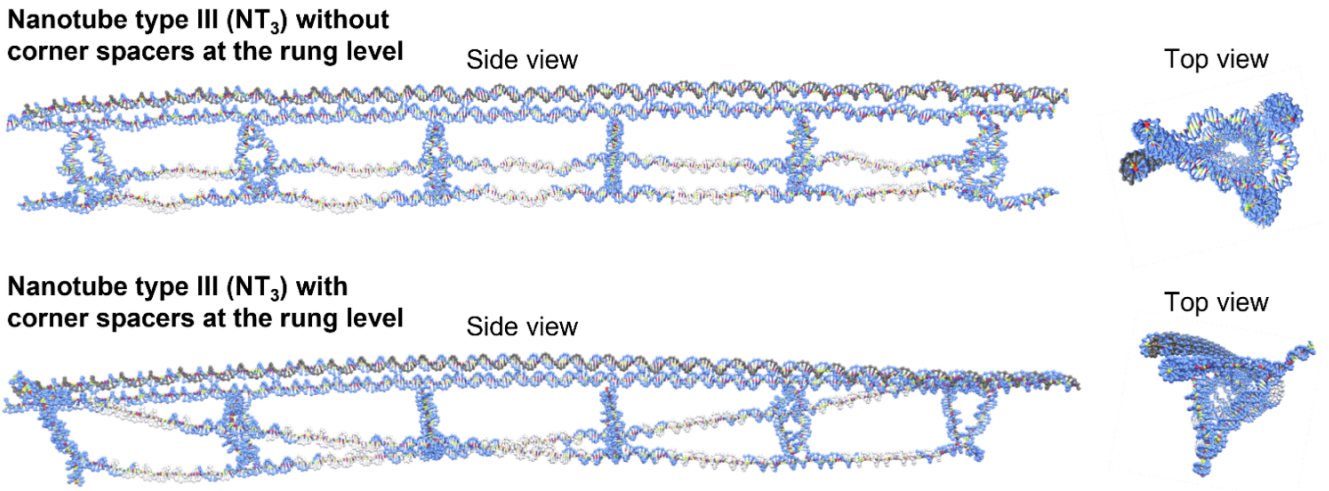

Figure S24. MD simulation of size defined DNA nanotube type III assembled with flexible and rigid rung units. Addition of spacers at the corner of each sequence hybridizing to the circular template (orange, blue, and red strands, **Figure S5**) induce an angular twist of 100^{o} between the first and sixth rung units (bottom panel) but the lack of these spacers results in no angular twist (top panel).

In our design, the core rung units feature sticky ends from the top and bottom, as shown in Figure 1 (B), indicating that the maximum number of linking strands that can hybridize per rung unit is two. Therefore, we varied the linking strands equivalents with respect to the rung unit to include the following ratios, 1 to 1 eq., 1.25 to 1 eq., 1.5 to 1 eq., and 2 to 1 eq. One set of nanotubes from each of the categories (NT_1, NT_2, and NT_3) was chosen, and the assembly was performed using the assembly protocol described in section 6 of the supporting information. Native PAGE analysis revealed the presence of a non-penetrating band that corresponds to the nanotube and a band with a higher mobility shift corresponding to the linking strands (**Figure S25**). Adding a one-to-one ratio of linking strands to rung units reveals no leftover linking strands, whereas higher equivalent ratios reveal an excess of linkers that didn't bind to the nanotube. This experiment indicates the independence of the linking strands

equivalents of the nanotube formation even if tubes with different degrees of flexibility are being assembled.

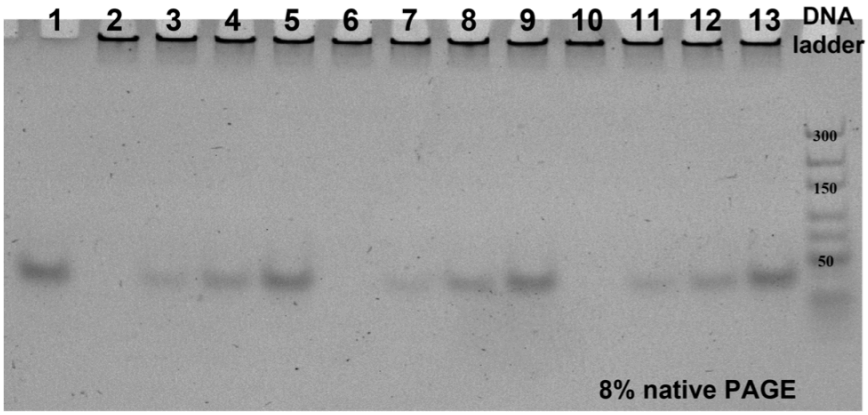

Figure S25. Dependence of DNA nanotube formation on the equivalent number of linking strands. Lane 1 represents the partially double-stranded linking strands. Lanes 2 to 5 represent a 1:1, 1.25:1, 1.5:1, and 2:1 ratio of linking strands to **partial-ds-NT$_1$**. Lanes 6 to 9 represent a 1:1, 1.25:1, 1.5:1, and 2:1 ratio of linking strands to **ds-NT$_{2b}$**. Lanes 10 to 13 represent a 1:1, 1.25:1, 1.5:1, and 2:1 ratio of linking strands to **DX-NT$_3$**. O'GeneRuler Ultra Low Range DNA ladder is used.

Strand displacement strategy

The reversible switching between double- and single-stranded nanotubes type II was accomplished by erasing and refilling complementary strands of LS1, LS2, and the spacer strand 1a using strand displacement. This was accomplished by employing modified linking and spacer strands with a 10-base overhang to produce nanotubes at a concentration of 50 nM in 1xTAMg. After assembling these constructs, we added 5 equivalents of each fully complementary eraser strand and incubated the mixture overnight at room temperature. To determine if their double-stranded forms could be regenerated, the mixture was incubated overnight with 5 equivalents of 1a and LS1/2*.

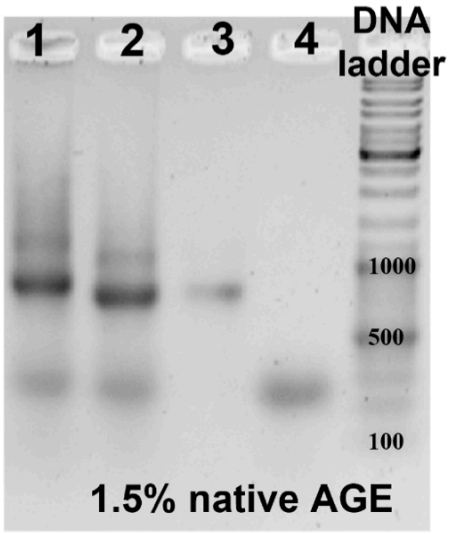

Figure S25. Native AGE characterization of the reversible switching between double-stranded and single-stranded nanotube type II. **ds-NT$_{2b}$** is assembled using modified linking and spacer strands with a 10-base overhang (lane 1). Incubation of the mixture with the fully complementary eraser strands yielded a product with a higher mobility shift (lane 2). Lanes 3 and 4 correspond to nanotubes formed with no linking strands and to the rung unit, respectively.

SI-7. Coarse-grained simulations of DNA nanostructures

OxDNA is a coarse-grained nucleotide-level model of DNA in which each nucleotide is a rigid entity with sites representing the backbone and base. The internucleotide interactions involve base stacking, a backbone potential, hydrogen bonding between complementary base pairs, electrostatic interactions between the charged backbones, excluded volume, interactions between the charged backbone and the cations present in solution, and cross stacking between diagonally opposite bases in double-stranded DNA. These have been tuned to mimic DNA structure, hybridization thermodynamics, and mechanical properties of double- and single-stranded DNA. The interactions that contribute to the oxDNA potential are discussed elsewhere.[1-2] On oxDNA.org, the job submission form requires two files: configuration and

topology. As a result, the DNA structural models created with vHelix[3] were transformed into oxDNA simulation-compatible files (.top and .dat)[4] using *tacoxDNA*.[5] The structures are then simulated using the publicly-available oxDNA website (oxDNA.org).[6] All simulations were conducted under standard conditions using 1×10^9 simulation steps at a temperature of 20 ^oC in a sodium chloride solution (1 M). OxView was used to examine simulation results and capture all images.[7] Following the simulation, we used the same website (oxDNA.org) to determine the mean position of each nucleotide and the root mean square fluctuation of each particle in relation to its mean position.

SI-8. AFM microscopy

AFM imaging was performed in ambient air using a MultiMode8™ SPM linked to a Veeco Nanoscope™ controller. ScanAsyst-Air triangular silicon nitride probe (k = 0.4 N/m and f_o = 70 kHz; Bruker) was used to acquire images in tapping mode. All images were collected at a 1 Hz scan rate with a 512 x 512-pixel resolution. All samples were diluted in 1xTAMg to a concentration ranging from 1 to 10 nM. 4 µL of the sample was placed onto a newly cleaved mica surface and kept at room temperature for 30 seconds to allow DNA to adsorb, followed by three rounds of washing with 40 µL of filtered autoclaved water. Following the final round of washing, the residual liquid was removed using a vigorous stream of compressed air, and the samples were dried for at least 30 minutes under vacuum prior to imaging. NanoScope Analysis 1.40 was used to examine the images, and flattening was utilized to adjust for tilt, bow, and scanner drift. All AFM images were taken for the crude nanotubes without any additional purification.

SI-9. References

1. Snodin, B. E.; Randisi, F.; Mosayebi, M.; Šulc, P.; Schreck, J. S.; Romano, F.; Ouldridge, T. E.; Tsukanov, R.; Nir, E.; Louis, A. A., Introducing improved structural properties and salt dependence into a coarse-grained model of DNA. *The Journal of chemical physics* **2015,** *142* (23), 06B613_1.
2. Ouldridge, T. E.; Louis, A. A.; Doye, J. P., Structural, mechanical, and thermodynamic properties of a coarse-grained DNA model. *The Journal of chemical physics* **2011,** *134* (8), 02B627.
3. Benson, E.; Mohammed, A.; Gardell, J.; Masich, S.; Czeizler, E.; Orponen, P.; Högberg, B., DNA rendering of polyhedral meshes at the nanoscale. *Nature* **2015,** *523* (7561), 441-444.
4. Snodin, B. E. K.; Randisi, F.; Mosayebi, M.; Šulc, P.; Schreck, J. S.; Romano, F.; Ouldridge, T. E.; Tsukanov, R.; Nir, E.; Louis, A. A.; Doye, J. P. K., Introducing improved structural properties and salt dependence into a coarse-grained model of DNA. *The Journal of Chemical Physics* **2015,** *142* (23), 234901.
5. Suma, A.; Poppleton, E.; Matthies, M.; Šulc, P.; Romano, F.; Louis, A. A.; Doye, J. P. K.; Micheletti, C.; Rovigatti, L., TacoxDNA: A user-friendly web server for simulations of complex DNA structures, from single strands to origami. *J. Comput. Chem.* **2019,** *40* (29), 2586-2595.
6. Poppleton, E.; Romero, R.; Mallya, A.; Rovigatti, L.; Šulc, P., OxDNA.org: a public webserver for coarse-grained simulations of DNA and RNA nanostructures. *Nucleic Acids Res.* **2021,** *49* (W1), W491-W498.
7. Poppleton, E.; Bohlin, J.; Matthies, M.; Sharma, S.; Zhang, F.; Šulc, P., Design, optimization and analysis of large DNA and RNA nanostructures through interactive visualization, editing and molecular simulation. *Nucleic Acids Res.* **2020,** *48* (12), e72-e72.